

A REVIEW OF AERODYNAMICALLY INDUCED FORCES ACTING ON CENTRIFUGAL COMPRESSORS, AND RESULTING VIBRATION CHARACTERISTICS OF ROTORS



by

D. Fred Marshall

Manager of Product Engineering

Dresser-Rand Company

Le Havre, France

and

James M. Sorokes

Team Leader, Applied Aerodynamics Group

Dresser-Rand Company

Olean, New York



D. Fred Marshall is presently the Manager of Product Engineering at Dresser-Rand's Operation in Le Havre, France. He has been involved in the design, development, and analysis of industrial turbomachinery for more than 30 years at Turbodyne Corporation, the Dresser Clark Division of Dresser Industries, the General Electric Company, and the Dresser-Rand Company. Mr. Marshall joined the Turbo Products Division of Dresser-Rand

Company in 1990 as Manager of Engineering Sciences. He has authored four technical papers, and holds four patents.

Mr. Marshall received his B.S. degree (Mechanical Engineering, 1969) from the University of Rochester (1969) and his MBA degree from St. Bonaventure University (1979).



James M. Sorokes has been employed at Dresser-Rand (formerly Dresser-Clark) for 24 years, all of those in the Aerodynamics Group, in Olean, New York. He has held various supervisory positions since 1984 and is currently the team leader of the Applied Aerodynamics Group. In this capacity, he is responsible for the development, design, and analysis of all rotating and stationary aerodynamic components of centrifugal compressors.

Specific areas of concentration include single stage rig testing, aeromechanical phenomenon (i.e., rotating stall), practical application of CFD, alternate design philosophies and techniques, etc.

Mr. Sorokes received a B.S. degree from St. Bonaventure University (1976). He is a member of AIAA, ASME, and the ASME Turbomachinery Committee. He has authored or coauthored more than 20 technical papers and has been an instructor at various seminars and tutorials at Texas A&M University and Dresser-Rand. He also holds two U.S. patents.

ABSTRACT

There are several sources of nonsynchronous forced vibration of centrifugal compressor rotors. Many of them are aerodynamic phenomena, created within the gas path of the compressor. Phenomena such as impeller stall, diffuser stall (with and without

vanes), and flow instabilities caused by impeller to diffuser misalignment, are all characteristic flow disturbances that can cause forced vibration. In fact, often the only indications of these phenomena are found in the resulting rotor vibration signals.

Several phenomena that can cause nonsynchronous vibration are reviewed, and for each one background information, as well as detailed descriptions of the flow field, or other source of the excitation, is provided. This includes the use of computational fluid dynamic (CFD) analytical results to describe the flow where applicable.

The review also includes, when available, dynamic pressure transducer test data that can be used to verify the presence of the phenomena, and rotor vibration data indicating the presence of such phenomena. This includes test data of actual machines, indicating characteristics such as frequency and amplitude.

INTRODUCTION

This discussion centers on forced vibration of rotors, the sources and reasons for the forces involved, and the resulting vibration characteristics as might be revealed by noncontacting rotor probes. To adequately cover this information, we must start with a basic description of rotor vibration characteristics, and the response of rotors to various types of excitation. Once this is complete, our discussion will move on to descriptions of the causes of each of the phenomenon of interest, and then to the resulting vibration signals.

Fortunately, the primary rotor vibration characteristics of interest can generally be illustrated by reference to simple models. This allows us to describe them without resorting to involved differential equations and their solutions. The description of the causes of the forcing phenomena is much more specific to centrifugal compressors, as opposed to rotors in general. Here, the forces that can be generated within the gas path are described, and the reasons for those forces are covered in detail. In some cases there are data available regarding the dynamic pressure fields created by these phenomena, and where it is available, it has been included.

The resulting rotor vibration signals are the primary way we can become aware of these forcing functions. With an understanding of how rotors respond to forces, and the potential forcing functions they may encounter, the recognition of vibration due to such phenomena becomes simpler than it otherwise may be.

VIBRATION CHARACTERISTICS

As noted above, we are fortunate that the vibration characteristics of interest can be described using simple one degree of freedom systems. The material below describing those characteristics could be extracted from most vibration texts, such as those

listed in the bibliography. It has simply been condensed and described in a manner that is most relevant to the particular problem of rotors.

Free Vibration

Free Vibration Without Damping

For our purposes, the simple spring-mass system, as depicted in Figure 1, can be used for much of our discussion of the features of interest for a rotor system undergoing free vibration. Equation (1), the equation of motion for this simple system, produces the general solution defined by Equation (2).

$$m\ddot{x} + kx = 0 \tag{1}$$

$$x = X \sin(\omega_n t + \Phi) \tag{2}$$

$$\omega_n^2 = k/m \tag{3}$$

where:

- m = Mass
- \ddot{x} = Acceleration
- k = Spring coefficient
- x = Position/amplitude
- X = Maximum position/amplitude
- ω_n = Natural frequency
- t = Time
- Φ = Phase angle

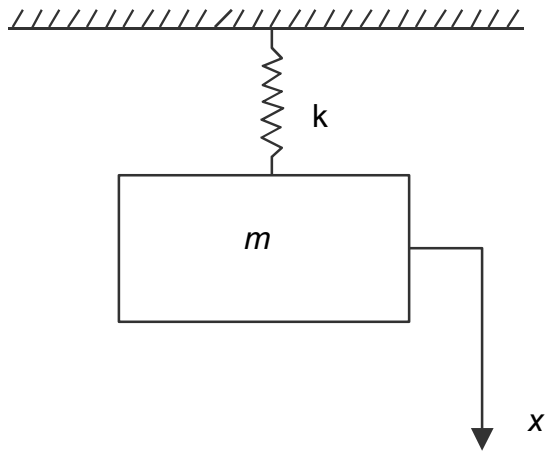


Figure 1. Simple Spring-Mass System.

In the absence of damping or external forces, once such a system is moved from its equilibrium position, the vibration as described by the equations continues forever, at the harmonic frequency defined by Equation (3).

Free Vibration With Damping

The situation can both be complicated slightly, and made much more realistic, by adding (viscous) damping. For the purposes of this discussion, the simple one degree of freedom spring-mass-damper system, as depicted in Figure 2, can be used to describe the features of interest for a rotor system with damping undergoing free vibration. Equation (4) is the equation of motion for this simple system.

$$m\ddot{x} + c\dot{x} + kx = 0 \tag{4}$$

$$C_{cr} = 2\sqrt{km} \tag{5}$$

$$x = Xe^{-\mu t} \cos(pt + \Phi) \tag{6}$$

where, in addition to the definitions above:

- c = Damping coefficient
- \dot{x} = Velocity
- C_{cr} = Critical damping
- p = As defined below
- μ = As defined below

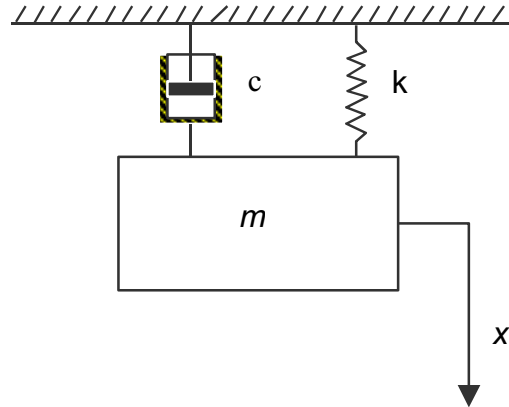


Figure 2. Simple Spring-Mass-Damper System.

If critical damping is defined by Equation (5), and one investigates only the case where damping is less than critical, then a solution is generated as defined by Equation (6). This solution has a harmonic component ($\cos(pt + \Phi)$) with a natural frequency given by (pt , where $p = \sqrt{\omega_n^2 - \mu^2}$ and $\mu = \frac{c}{2m}$), and a decaying component ($e^{-\mu t}$), with the rate of decay determined by the coefficient in the exponent (μ). With any given initial position not at the equilibrium position of the system, the value of this exponent determines the rate at which the vibration of the system will return to zero. The coefficient over one period of vibration (μT , where T is one period) is called the logarithmic decrement (log dec), and it is defined by Equation (7).

$$\delta = \mu T \tag{7}$$

It is therefore evident that whether or not there is any damping in the system, the system in free (unforced) motion will vibrate only at its natural frequency. The amplitude is completely defined by the motion at the natural frequency, and if damping is present, the log decrement defines the rate of decay.

Forced Vibration

While there are several types of forces that can act on compressor rotors, they all can be characterized as either periodic or nonperiodic (arbitrary). First harmonic forces will be discussed, a subset of periodic forces. The more general case of periodic forces is then covered, followed by arbitrary forces.

Harmonic External Forces

Harmonic external forces can be represented by a simple sine wave. The force is of the form shown in Equation (8), and results in an equation of motion for a damped single degree of freedom system as shown in Equation (9). We get a general solution of the form in Equation (10). As shown by Equation (11), for a given relative force level ($D = F/k$) the amplitude is dependent on the relative location of the forcing function frequency to the system natural frequency ($\tau = \omega/\omega_n$), as well as the amount of damping in the system ($\rho = \frac{c}{2m\omega_n}$). As Equation (10) shows, the frequency of the vibration is at the frequency of the forcing function, not the system natural frequency. At low levels of damping, it is also apparent from Equations (10) and (11) that the amplitude response

to the force would approach infinity as the forcing function frequency approaches the system natural frequency. This is the familiar concept of resonance.

$$s(t) = F \cos(\omega t) \quad (8)$$

$$m\ddot{x} + c\dot{x} + kx = F \cos(\omega t) \quad (9)$$

$$x = P \cos(\omega t - \Phi) \quad (10)$$

$$P = \frac{D}{[1 - \tau^2]^2 + (2\rho\tau)^2}^{1/2} \quad (11)$$

where, in addition to the earlier definitions:

$s(t)$ = Harmonic forcing function

ω = Forcing function frequency

F = Maximum of forcing function

P = Maximum of response amplitude

It is therefore evident that the steady-state response of a system to a harmonic forcing function is harmonic motion at the same frequency as the force, with maximum amplitude occurring when the system natural frequency is in resonance with the forcing function.

Periodic External Forces

A periodic force is not a clean sine wave, but it does repeat itself over some time period, with a frequency of ω . In that case, the forcing function may be expanded in a Fourier series, and the force is described in the form of Equation (12). Any periodic signal can be expanded in this way, and this capability can be used every time we look at vibration spectrum data. It is this characteristic that allows a fast Fourier transform (FFT) analyzer to translate a vibration signal such as that shown in Figure 3 into the frequency domain, as in Figure 4.

$$s(t) = \sum_1^{\infty} F_n \cos(n\omega t + \theta_n) \quad (12)$$

$$x = \sum_1^{\infty} P_n \cos(n\omega t + \theta_n - \phi_n) \quad (13)$$

$$P_n = \frac{D_n}{[(1 - n^2\tau^2)^2 + (2\rho n\tau)^2]^{1/2}} \quad (14)$$

where, in addition to the earlier definitions:

F_n = The nth multiple of the force

n = The nth multiple

θ_n = The phase angle related to the nth multiple force

P_n = The maximum of the nth multiple position/amplitude

ϕ_n = The phase angle related to the nth multiple amplitude

D_n = The relative force level of the nth multiple

The steady-state response of a simple spring-mass system to a force in the form of Equation (12) is shown by Equation (13). This indicates the vibration occurs at the frequency of the forcing function and its multiples (often called harmonics, and not to be confused with the harmonic forcing function mentioned above). As shown by Equation (14), the amplitude is maximized when the base forcing function frequency, or any of its multiples, equals the system natural frequency. It is then apparent that the response of a system to a periodic external force can be analyzed by decomposing the forcing function into its components (Fourier series), and then analyzing the response of the system to each of those components. The total response of the system is given by the sum of the individual responses, which can be looked at as harmonic forces, as described earlier.

Arbitrary, or Nonperiodic, External Forces

Arbitrary, or nonperiodic, external forces are transient in nature, and the most common way to investigate them is to consider an

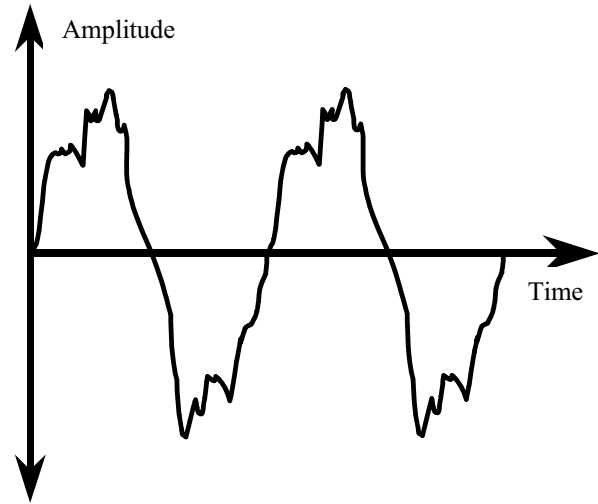


Figure 3. Periodic Signal.

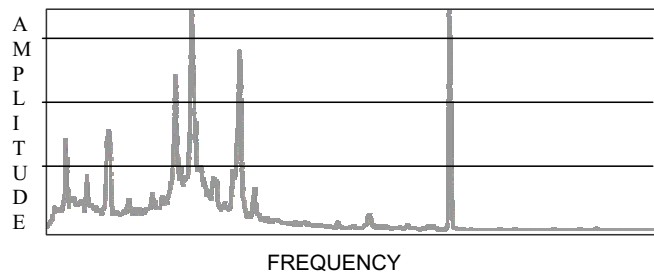


Figure 4. Frequency Spectrum from Periodic Vibration Signal.

impulse force. An impulse is typically a force of significant magnitude that acts for a short but finite time, and can be represented by an equation of the form in Equation (15). When a simple spring-mass system is excited by such an impulse, it responds in free vibration with initial conditions of ($x = 0$) and ($\dot{x} = F/m$). This results in vibration as represented by Equation (16), which can be seen to be at the system natural frequency, with an amplitude linearly related to the magnitude of f .

$$f = \int_t^{t+\epsilon} F dt \quad (15)$$

$$x = \frac{f}{m\omega_n} \sin\omega_n t = f g(t) \quad (16)$$

where, in addition to the earlier definitions:

f = The unit impulse force

F = The impulse force amplitude

$g(t)$ = Response to the unit impulse force

Using the principle of superposition, excitation due to arbitrary external forces, as depicted in Figure 5, can be treated as a series of impulses. The resulting response is defined by a superposition integral, in the form of Equation (17).

$$x = \int_0^t f(t')g(t-t')dt' \quad (17)$$

This means the general response of the system would be expected to be movement due to the forces themselves, plus vibration at a natural frequency, with varying amplitude levels, depending on the timing of the impulses. The relationship of any new impulse force to the existing vibration would determine the resulting vibration.

Summary

The above description points out an important distinction between different types of forced vibration. Purely harmonic

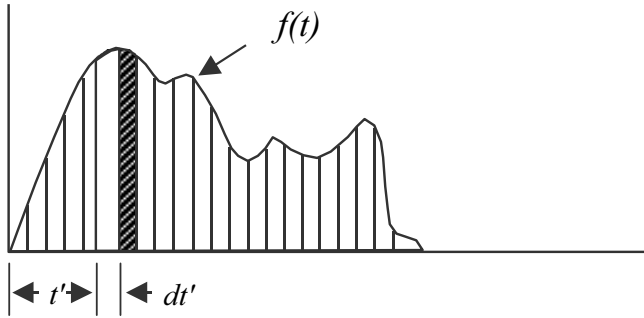


Figure 5. Force Due to Series of Impulses.

forcing functions will result in vibration at the frequency of the force, with the amplitude depending on the level of force and the proximity of the forcing frequency to the system natural frequency. The more general form of periodic forcing functions will result in vibration at the frequency of the force, plus its multiples, with the amplitude again dependent on the level of the force, plus the proximity of the forcing frequency, or any of its multiples, to the system natural frequency. In contrast, vibration due to a nonperiodic, or arbitrary forcing function, will occur at the system natural frequency. The amplitude at that frequency will vary, and other movement in response to the forces will appear as random amplitudes and frequencies in the spectrum.

APPLICATION TO ROTOR VIBRATION

A compressor rotor can be considered as a special type of multi degree of freedom system. As such, it can exhibit both free vibration and forced vibration. Free vibration takes place when the system vibrates due to forces inherent in the system itself. This vibration always takes place at one or more of the natural frequencies of the system. Forced vibration occurs due to external forces. If this force is periodic, as it often is, the system will vibrate at some combination of the frequency of excitation and its multiples, with amplitudes dependent on the position of the excitation frequencies to the system natural frequencies. For nonperiodic forces, the response of the system will again be at some combination of its natural frequencies. The following should illustrate these characteristics in more detail.

Free Vibration

Free Vibration Without Damping

If one has a multi degree of freedom system, such as a compressor rotor, the above basic principles still apply. The system is more complicated, but has the same basic components. For calculation purposes, the mass is represented by the modeled rotor stations, and the spring is represented by stiffness matrices between mass stations on the rotor, and by stiffness coefficients at the bearing locations. A typical rotor system model for an undamped model of this type might look like Figure 6 without the damping (C).

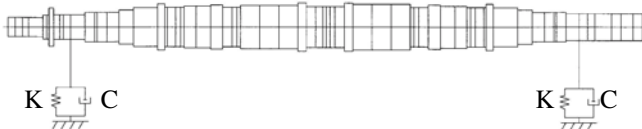


Figure 6. Rotor System Model.

For each degree of freedom in this model, there will be an (undamped) natural frequency. Such a model can therefore be used to generate the familiar critical speed map, as shown in Figure 7, where these frequencies vary with the spring coefficient applied at the bearing location. Each of these natural frequencies also has a

mode shape. These describe the way the rotor vibrates when at the particular natural frequency in question. The first four of these mode shapes for a typical beam style compressor would be as depicted in Figure 7. The result is a rotor system that has multiple natural frequencies, or principal modes. When undergoing free vibration, the overall vibration of the system is always some superimposed combination of these modes.

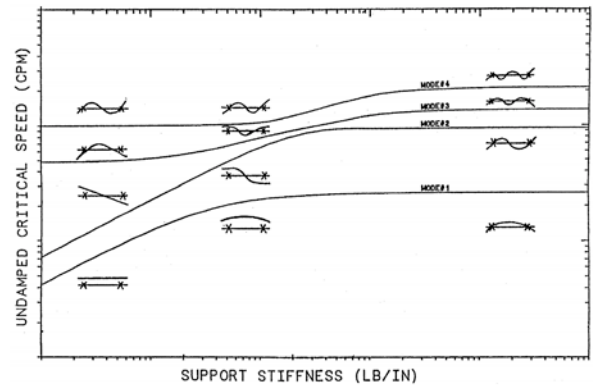


Figure 7. Critical Speed Map.

Free Vibration With Damping

Again, in a multi degree of freedom system, such as a compressor rotor, the basic principles discussed above still apply. With damping, the system becomes more complicated, but still has the same basic components. For calculation purposes, the rotor is represented by the modeled rotor stations, with the spring and damper represented by stiffness and damping coefficient matrices at any bearing and seal locations. A typical rotor system model might look like the one in Figure 6 but spring and damping coefficients in multiple directions are considered at each bearing, seal or other support point, as shown in Figure 8.

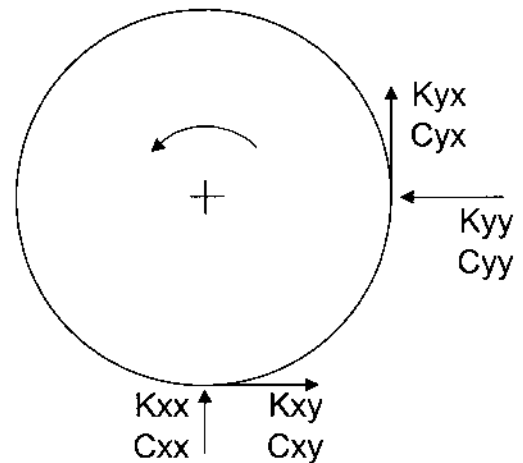


Figure 8. Cross-Coupling Coefficients.

For each degree of freedom in this system, there will be a damped natural frequency, often called an eigenvalue, again with a corresponding specific mode shape, and also with a logarithmic decrement. Each eigenvalue has its own decay rate, as defined by the log dec, which can therefore be used as a measure of available damping. The result is a rotor system that has multiple natural frequencies (eigenvalues), each of them having a specific mode shape and an amount of damping indicated by the log dec. Just as in the undamped case, the overall free vibration of this system will always be some combination of all the natural frequencies, and therefore of all the mode shapes.

Since, in the absence of any external forcing function, the vibration of a system such as a rotor can only occur at its natural frequencies, the dominant frequency of any vibration signal must be one of these natural frequencies. The result is a very clean vibration signal at typically one of these frequencies, with an amplitude that can be substantial.

In the real world, the situation most closely resembling such free vibration is rotor instability, where a mode (typically the first, or fundamental) is caused only by the "passive" excitation, represented by the spring and damping coefficients shown in Figure 8. This same figure can also be used to illustrate that "cross-coupling" coefficients (such as k_{xy}) can drive the rotor in a whirling motion.

Analytical techniques used to examine rotor stability can create an "unstable" rotor model mathematically simply with these coefficients at the bearing and seal locations. External forces are not needed. The term passive is used because forces are only generated in response to movement of the rotor, creating a self-generating mechanism. The term instability is used because with the right coefficients, the log dec of the mode of interest can go to zero, or below, creating an unstable situation, with a constantly increasing amplitude. The vibration is unbounded, until nonlinearity takes over (often as in contacting the bearing or seal).

The characteristics of rotor "instability" are therefore a clean, single frequency signal, occurring at the rotor natural frequency, with an amplitude that increases until bounded by other constraints. This type of subsynchronous vibration can be a serious problem. It can cause severe damage. Fortunately, it is not as commonplace as it once was. There are other reasons for compressors to vibrate at subsynchronous frequencies, however, and that is the primary topic of the rest of this discussion.

Forced Vibration

Harmonic Forces

An obvious instance of a harmonic force on a rotor is unbalance. For analysis, the rotor model adds a rotating force, as shown Figure 9. Its frequency is obviously equal to running speed, and the familiar amplitude versus speed plots can be produced, as shown in Figure 10, to measure response of the rotor to this external force. Since we are dealing with a multiple degree of freedom system, the vibration mode shape will vary depending both on how close the speed (forcing function frequency) is to the various natural frequencies, and the location of the unbalance. The location used for measuring vibration introduces another variable, since the mode shape at any given frequency will determine whether a particular probe location can be used to adequately measure response of the rotor. Similarly, asynchronous response analysis of a rotor to reduced frequency excitation can provide some picture of a rotor's ability to withstand a specific subsynchronous harmonic force.

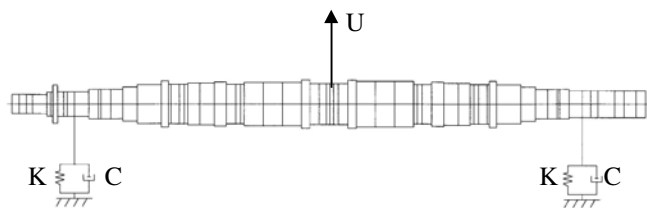


Figure 9. Rotor System Model Showing Unbalance Force.

A vibration signal due to a consistent harmonic external force would therefore be expected to be a steady vibration, with an amplitude dependent on the force and the proximity to a rotor natural frequency. This characteristic would result in a resonance at each natural frequency that becomes coincident with the force. If the frequency of a subsynchronous force changes, the vibration

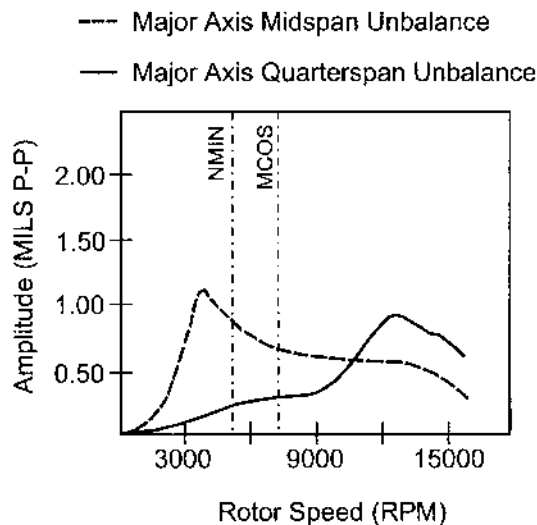


Figure 10. Amplitude Versus Speed Plot.

response frequency will also change, with the amplitude rising and falling depending on the proximity to the natural frequencies of the rotor. For a given system, with a given forcing function, one therefore has a relatively stable situation, with essentially no tendency to exhibit sporadic high vibration levels.

Periodic Forces

Nonsynchronous forces acting on rotors are generally in the form of aerodynamic forces. When these aerodynamic forces are periodic, they may or may not be harmonic, as well. A response plot similar to Figure 10 could again be used to examine the asynchronous response of the rotor to the force, or any multiples it may have. From the discussion above on periodic forcing functions, it is apparent that at frequencies below a given natural frequency of the system, both the force and any of its multiples can excite that mode if they are either in resonance, or close to resonance, with the natural frequency. On the other hand, periodic forces at higher frequencies cannot be in resonance with lower natural frequencies.

Just as for a single degree of freedom system, any vibration due to such forces will be at frequencies equal to the forcing function frequency, plus any integer multiples. The amplitude will vary as the frequency varies, depending on the proximity of the frequencies to rotor natural frequencies, and resonance can occur with any of the natural frequencies and the forcing function or any of its multiples. Again, for a given system under given conditions, this type of vibration is stable, consistent, and repeatable.

Arbitrary Forces

Arbitrary external forcing functions seen by compressor rotors are generally caused by transient aerodynamic activity. Since they act as an impulse force, however, they may also cause vibration at frequencies other than one of the rotor's natural frequencies. However, the reaction of a rotor to aerodynamic activity that can cause transient arbitrary forces is not generally analyzed, since the potential characteristics and locations of the forces involved are innumerable. It is then left to evaluation of vibration signals to determine potential causes of vibration, and whether they should cause any concerns.

Just as with a single degree of freedom system, arbitrary forcing functions can cause vibration at one or more of a rotor's natural frequencies. The amplitude at the natural frequency will vary, however, as the amplitudes of the various impulses vary. Other movement of the rotor due to the impulse forces would appear as random frequencies and amplitudes on a signal analyzer. Steady vibration at any frequency will not occur, however. This type of

forced vibration can therefore be separated from unforced “instability” when evaluating vibration data most readily by viewing real time signals, to separate relatively steady or constantly increasing vibration from unsteady vibration at multiple frequencies. In real time, amplitudes and frequencies will constantly vary, with natural frequencies being the most prominent in most instances. Vibration levels will be determined by the stiffness and damping of the system, and the amplitude of the forces applied.

One can see from these results that unforced subsynchronous vibration (instability) will be a relatively clean signal at the rotor natural frequency. Forced subsynchronous vibration due to a harmonic force will be a clean single frequency that is often not at a rotor natural frequency. Forced subsynchronous vibration due to a periodic force will be at a frequency and its multiples, again usually not at a rotor natural frequency (although the existence of multiples increases the chance of resonance). Finally, forced subsynchronous vibration due to arbitrary (impulse) forces will be at multiple, and continuously varying frequencies and amplitudes, with maximum amplitudes usually occurring near rotor natural frequencies. With this basis, it is useful to describe the causes of some of the harmonic, periodic and arbitrary forces that can create such vibration signals.

AERODYNAMIC FORCES

Definitions

Before further discussions on the aerodynamic forces, a definition of four terms must be presented so that there is no confusion as to their interpretation in this document. Those terms are surge, stall, rotating stall, and hysteresis zone and they are defined as follows:

- **Surge**—is a system phenomenon that is not only dependent on the compressor but on all components of the process; i.e., piping, valves, pressure vessels, volumes, etc. Surge is defined as an operating condition at which full flow reversal occurs; i.e., flow progresses backward through the compressor section or stage and comes out the inlet. (Note, it is possible for one stage within a compression section to surge without the entire section surging.) It is typically accompanied by high radial and axial vibrations as well as extreme fluctuations in inlet and discharge pressure and temperature.
- **Stall**—A more localized phenomenon than surge, stall occurs when there is a localized region of reverse flow, reduced velocity/momentum, depressed pressure, etc. Stall can occur within a component of a stage and is frequently accompanied by an increase in subsynchronous vibration as well as pressure pulsations and a possible reduction in stage pressure rise. It is important to note that stall can occur at any point on a compressor operating map but is more common at very high or very low flow rates.
- **Rotating stall**—refers to that class of stall cells that rotate about the compressor; typically in the circumferential direction. The term is borrowed from the axial compressor world where it referred to the progression of a stall cell (or cells) from one rotor passage to the next. In the centrifugal world, it encompasses any stall cells that move relative to the stationary frame of reference. However, it is most commonly associated with impellers or diffusers.
- **Hysteresis zone**—When reducing flow, a phenomenon will appear at some flow rate. The phenomenon does not disappear simply by moving back above that flow rate. Instead, the flow rate has to be increased significantly beyond the onset rate to “wash out” the stall cells (Figure 11).

It is important to understand the distinction between surge and stall (or rotating stall). Quite often, turbomachinery engineers and users misinterpret or misuse these terms, leading to confusion as to which of the phenomena are happening in a compressor. Much of this confusion results from the common practice of labeling a

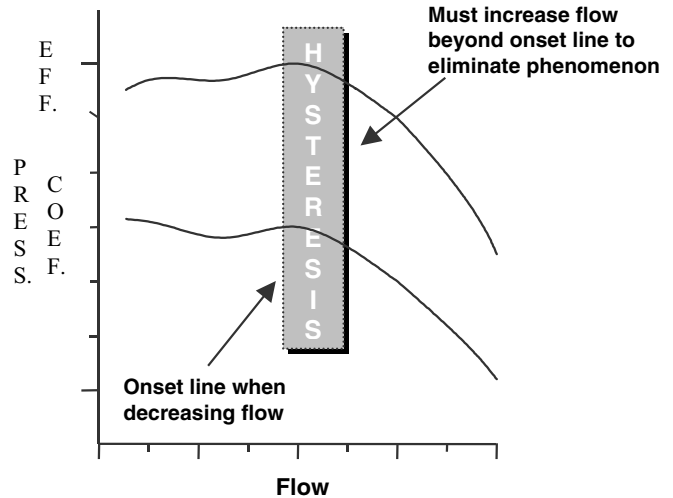


Figure 11. Hysteresis Zone.

compressor’s minimum stable flow rate as the “surge line” (Figure 12). In fact, the minimum flow rate shown on most as-tested performance maps is dictated by stall rather than surge. Stall or rotating stall tends to be a precursor to true surge. That is, as the inlet flow is reduced, the compressor will experience stall before it encounters a full flow reversal or surge. In some compression systems, the flow increment between the onset of stall and the onset of true surge is very small and it may be impossible to detect the stall without encountering full surge. In other systems, there is a significant difference in the flow rates at which stall and surge occur.

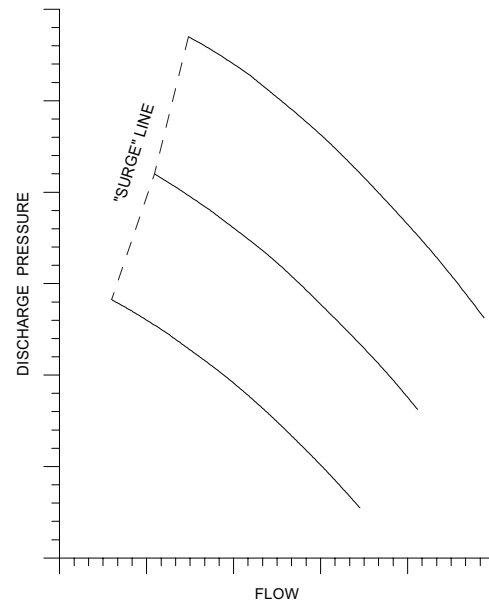


Figure 12. Compressor Map Showing “Surge” Line.

No further commentary will be offered on the system phenomenon, surge. Rather, the discussion will center on stall and, in particular, impeller and vaneless diffuser rotating stall.

Stationary Stall

Before addressing rotating stall, a few comments are warranted on the stationary form. Stationary stall cells may or may not have detrimental effects on compressor aerodynamic and mechanical performance. Much like its rotating counterpart, stationary stall causes nonuniform pressure fields or unbalanced forces that can

influence the compressor rotor. Stationary stall cells can form in vaned diffusers, return channels, guidevanes, near volute tongues, etc. The most common factor that promotes the formation of stationary stalls is high levels of incidence (i.e., the difference between the gas approach angle and the vane setting angle, Figure 13). High incidence occurs as a compressor or compressor stage is operated far from its nominal or design flow condition; that is, near surge or in overload. The separation cells create pressure disturbances that influence other upstream or downstream stage components. For example, the impeller shown in Figure 14 would be affected by the nonuniform pressure field caused by the flow separation from the diffuser vanes. The interaction of the impeller with this nonuniform field may be evidenced by an increase in vibration at blade-vane passing. Obviously, diffuser vane angles must be set accurately to ensure that high incidence and the resulting separation will not arise within the compressor's required operating map.

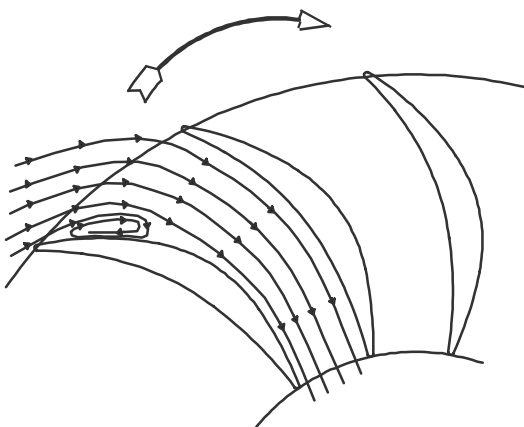


Figure 13. Stationary Stall Cell in a Return Channel.

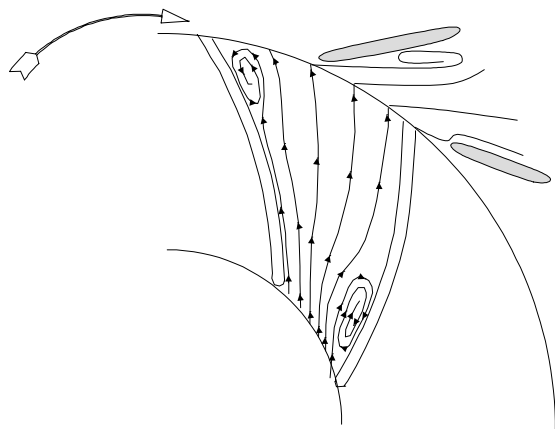


Figure 14. Sketch of Flow Separation in Impeller Due to Interaction with Separated Diffuser.

Stationary stall formation can also occur when flow encounters very tight curvatures. If curvature radii are too small in a return bend, guidevane, on a return channel vane, etc., the flow separates from the highly curved surface and a stall cell can form. Misalignment of parts in a compressor flowpath can also cause the flow to separate or stall. All these phenomena might induce rotor

vibrations or contribute to such by prompting the formation of rotating stall. For example, if stationary stall cells form in a return channel or guidevane passage, the stall may disturb the flowfield such that rotating stall would initiate in the downstream impeller. Therefore, stationary stall cannot be totally ignored as a possible contributor to rotor excitation. However, no further comments will be offered on the subject.

Rotating Stall

Rotating stall is best described as a nonuniform circumferential pressure field that rotates at a speed other than the compressor operating speed. The nonuniform pressure field might exert unbalanced forces on the compressor rotor, sometimes resulting in asynchronous vibrations. Since the rotational speed of the pressure field is most often lower than the rotor rotational speed, the vibration frequencies are subsynchronous.

As noted, the two most common forms are impeller and diffuser rotating stall. Both may have significant effects on mechanical and aerodynamic performance. In most compressors, rotating stall does not appear except at lower flow rates; i.e., very near surge. However, in some cases, they have been encountered very near design flow. Further complicating matters, some forms of "interaction stall" actually are more prevalent at the high capacity end of the performance map.

Confounding the situation even further, other components can produce forces that affect the rotor vibration signatures, approximating stall characteristics; i.e., seals and bearings. However, these rotor effects are typically not as sensitive to compressor operating conditions. Their response frequency is normally evident over the entire operating envelope and remains relatively constant despite changes in flow rate or discharge pressure. It is important to rule out such effects before attributing a subsynchronous rotor vibration to rotating stall.

Impeller Rotating Stall

Numerous researchers have investigated impeller rotating stall and there are equally numerous amounts of theories and opinions as to its nature and influences on compressor aeromechanical performance. Much of this work was drawn from or based upon studies done in the axial compressor world. However, the two early works that gained some notoriety in the centrifugal fraternity were those of Abdelhamid (1980) and Frigne and Van den Braembussche (1984). Their efforts sought to classify the various forms of rotating stall that could occur in a centrifugal stage.

Abdelhamid suggested that impeller rotating stall could result from flow perturbations at the impeller exit that would not allow the flow to follow the blading. These perturbations may be a consequence of disturbances within the impeller passages (i.e., separation cells, Figure 14) or strong interactions between the impeller and the diffuser (i.e., the diffuser walls interfering with the impeller exit area through misalignment of parts, etc.).

Frigne and Van den Braembussche also studied the characteristics of rotating stall (impeller and diffuser) and published a series of criteria that have been widely used to distinguish between the various types. Their study identified two distinct forms of impeller stall; abrupt and progressive. They also felt that the abrupt stall was the result of strong interactions between the impeller and diffuser while the progressive variety was more the consequence of the impeller flowfield itself. Their publication identified the frequency range for the two types as follows: Abrupt—26 percent to 31 percent of running speed; Progressive—67 percent to 82 percent of running speed.

Other researchers have identified the probable causes for progressive impeller rotating stall as:

- Flow separations near the impeller exit;
- Incidence angles at the impeller leading edge; or
- Pressure disturbances caused by the impeller blade geometry.

Based on a review of their published works, impeller rotating stall can manifest itself as frequencies from 26 percent of running speed up to 100 percent of running speed. It has also been suggested that some investigators confused diffuser stall as impeller stall. In short, though much has been published on the subject of impeller rotating stall and though many claim to have complete knowledge on the issue, the inconsistencies and contradictory nature of their guidelines, observations, and/or conclusions suggest that additional work is required before anyone can claim a total understanding of this phenomenon.

Impeller Rotating Stall Characteristics

Compressors experiencing impeller rotating stall can exhibit some or all of the following characteristics:

- The subsynchronous radial vibration frequency falls in the range of from 50 percent to 80 percent of the compressor running speed. Note: as suggested above, this range could be as large as from 26 percent to 100 percent of running, though the smaller range is more widely accepted.
- The subsynchronous vibration frequency tracks with running speed.
- There is normally no hysteresis zone associated with impeller stall. That is, there will be a very distinct flow rate at which the problem will come and go.
- It may be possible to throttle through the indications of stall such as subsynchronous vibration. That is, it may only occur over a limited flow band and disappear at lower flow rates. For example, when reducing flow rate, a subsynchronous vibration due to such a stall may arise at some Q/N. The vibration persists with further reduction in flow until a point is reached where it disappears.
- There may be a discontinuity or “droop” in the performance curve associated with the onset of the subsynchronous vibration.

Unfortunately, as noted, there is no consensus on the characteristics of impeller rotating stall. As such, it is difficult to provide definitive guidelines for its identification. However, there is good agreement on the various contributors to impeller stall; that is, geometric configurations or flow profiles to avoid. All also agree that detailed 2-D or 3-D analyses of the impeller and its associated hardware can identify potential sources for impeller rotating stall. However, how such stalls manifest themselves (i.e., characteristic frequencies) is still the subject of much debate.

Examples of Rotating Stall Attributed to Impellers

In the past, high flow coefficient stages have been more susceptible to impeller rotating stall. Some obsolete high flow impellers have shown a drooping trend in the pressure coefficient curve in the region between design and surge flow, especially when applied at high tip Mach number, U_2/A_o (Figure 15). This droop was accompanied by an increase in subsynchronous vibration at approximately 66 percent of the compressor running speed. Note that this frequency falls within the guidelines for impeller stall published by Frigne and Van den Braembussche (1984). Also, the general shape of the performance curve for these impellers agreed with the trends observed by the two researchers.

One-dimensional analyses on these obsolete impellers showed no obvious problems; i.e., relative velocity ratios, incidence levels, and various other parameters gave no indications that these impellers would suffer stall problems. Two-dimensional studies also yielded satisfactory results, i.e., loading parameters and velocity distributions fell within the generally accepted guidelines. However, when 3-D flowfield analyses (computational fluid dynamics (CFD)) were performed, some clear shortcomings were observed.

CFD analyses showed that large separation zones were forming in the impeller passages, prompted by high levels of turning both along the shroud and on the blading (Figure 16). These separation zones were coalescing into large wake regions at the impeller exit and

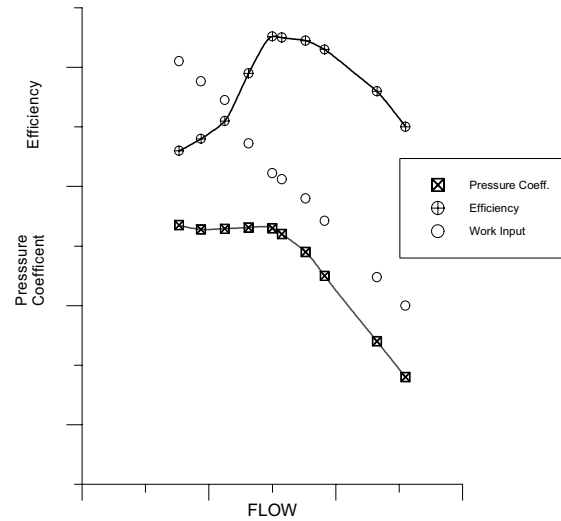


Figure 15. Data from Compressor Stage Experiencing Impeller Stall.

applying an excitation force to the rotor (Figure 17). Redesign of the impellers to an arbitrary bladed, full inducer configuration eliminated the stall and all related performance problems. These results were reported by Sorokes and Welch (1991) and Sorokes (1993). In light of the problems with these impellers, new guidelines to limit the amount of blade and cover turning were implemented.

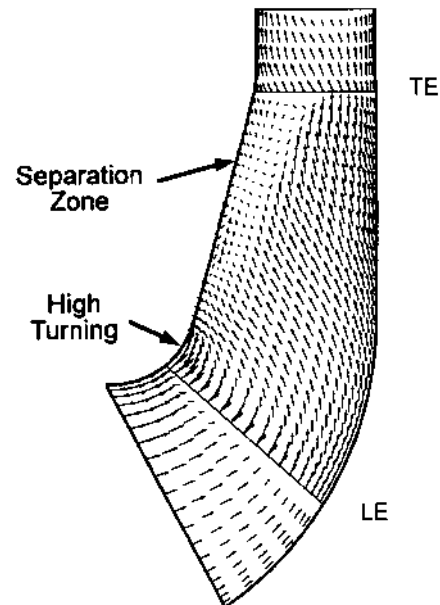


Figure 16. Impeller CFD Analysis Showing Separation Zone.

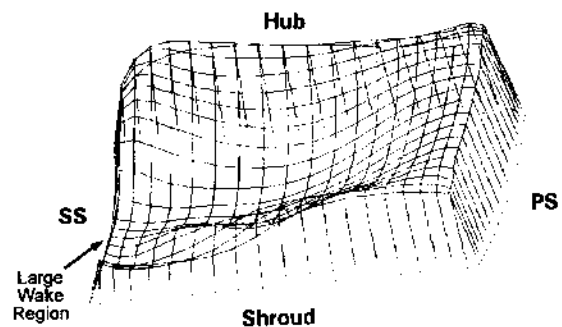


Figure 17. Impeller Exit Mach Number Distribution.

More recently, a novel form of impeller stall was experienced during full-load, full-pressure testing on a barrel compressor for high pressure gas reinjection. The unit exhibited subsynchronous radial vibration at 91 percent of running. Of significance, the subsynchronous only became apparent during the full-load, full-pressure testing. There was no indication of any vibration problems during the class III test; i.e., performed at reduced pressure, gas density, and horsepower. Adding to the peculiarity, the subsynchronous vibration only occurred when the second section of the compressor was operating in a very limited flow range (Figure 18). Also, there was absolutely no evidence of a problem in the performance of the compressor; that is, there was no discontinuity in the efficiency curve or head coefficient rise throughout the flow band in which the subsynchronous vibration occurred. It is important to note that all the impellers, diffusers, return channels, etc., had been used in numerous previous applications without incident. Further, 1-D reviews had been conducted on all impellers and diffusers to ensure that they conformed to the guidelines for rotating stall avoidance that were being applied at the time. In short, there was no reason to suspect a rotating stall problem.

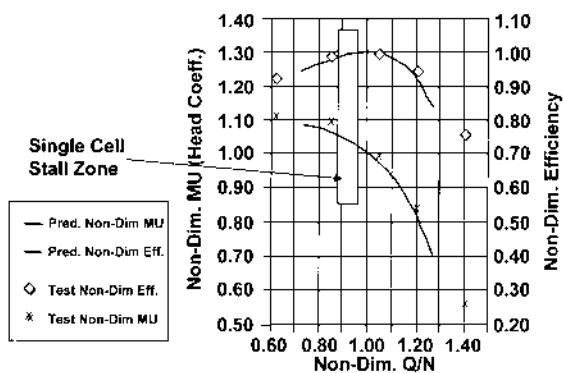


Figure 18. Performance Map Showing Apparent Impeller Stall Zone.

To identify the source of the excitation, dynamic pressure probes were installed in the diffusers and second section inlet. During the testing, pressure pulsations were discovered in the first and second stages of the second section that coincided with the onset of the subsynchronous radial vibration detected by the vibration probes (Figure 19). When throttling the compressor from design to lower flow rates, the pressure pulsations initiated at a frequency of 91 percent of running; i.e., exactly the same as the subsynchronous radial vibration frequency. With further reduction in flow rate, the pressure pulsation frequency changed to 182 percent of running speed. Coincident with this pulsation frequency change, the subsynchronous radial vibrations disappeared (Figure 20). With even further decreases in flow rate, the pressure pulsation frequency changed to 273 percent of running and then 364 percent of running, yet the subsynchronous radial vibrations never returned.

Dynamic pressure probes at the exit of one impeller clearly showed that, when the 91 percent of running vibration appeared, there was a single stall cell rotating at 91 percent of the rotor speed. This resulting unbalanced pressure force above the impeller caused the rotor response. When the stall mode shifted to two cells, the probes proved that the 182 percent of running pulsation was actually the result of two cells (180 degrees apart) rotating at 91 percent of running speed. Because the two pressure disturbances were diametrically opposing one another, the rotor forces were balanced. Similarly, when the 273 percent of running frequency was apparent, the result of three cells (120 degrees apart) rotating at 91 percent, the pressure forces on the rotor were again balanced (Figure 21).

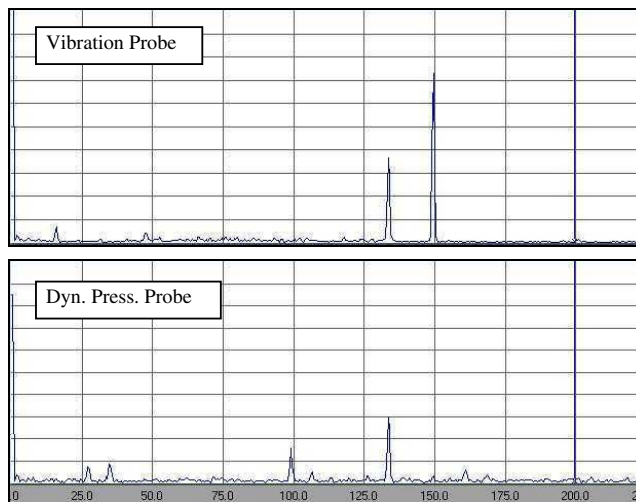


Figure 19. Spectra from Dynamic Pressure Probe and Vibration Probe During Impeller Rotating Stall.

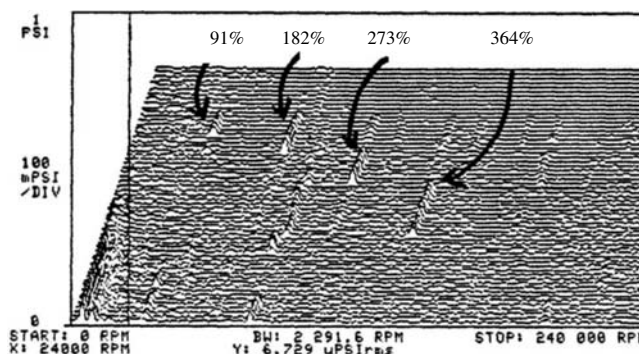


Figure 20. Waterfall Plot Showing Shift in Frequency with Flow.

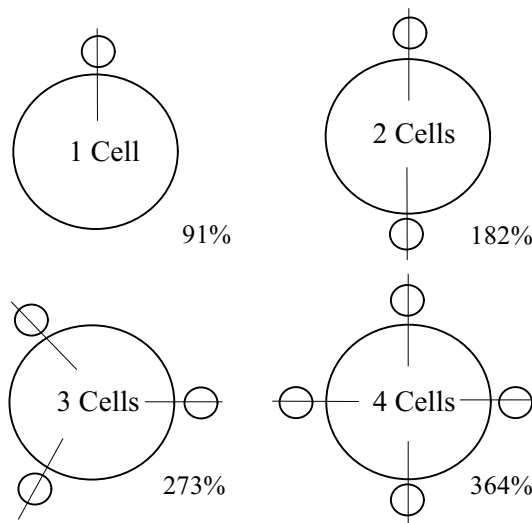


Figure 21. Orientation of Stall Cells.

The observed behavior of the rotating stall experienced in this compressor does not conform to any of the published characteristics for impeller stall and yet it was obvious that the impellers were creating (or at least amplifying) the phenomenon. In an effort to identify the root cause of the stall, a CFD study was conducted on the impellers. These analyses did show larger than normal amounts of secondary flow at the impeller exit. It was concluded that leading

edge incidence (though within prior experience with this impeller) and the aerodynamic loading on the blading were contributing to the high level of secondary flow. The impeller was redesigned to address these two issues and the problem was resolved.

The reason for providing so much detail on this case is that the original stage design adhered to all 1-D criteria existing at that time for stall avoidance and yet a problem occurred. Further, the stall's behavior was very unique and did not conform to any published material regarding the characteristics of rotating stall in centrifugal compressors. In short, this experience provided information on a form of impeller rotating stall not previously encountered. Clearly, more rigorous acceptance criteria were needed to properly assess the potential for centrifugal impeller rotating stall. Such criteria could not be based solely on simple 1-D calculations, though new 1-D guidelines were developed in light of this experience. The more obvious solution that was implemented was to make more effective (and frequent) use of 2-D or 3-D analyses.

Two more crucial observations must be made. First, as noted, the subsynchronous vibration was only evident when the compressor was run at full-load and full-pressure. Had only the class III test been done, the stall would not have been detected until the compressor was installed at the customer's site. Resolution in the field would have been far more difficult and time-consuming. Clearly, there are significant advantages to performing full-load, full-pressure testing prior to shipment of the compressor from the vendor's facilities.

Second, much of the research work done on rotating stall (impeller, diffuser, etc.) has been done using low pressure test vehicles; i.e., single-stage test rigs. As was seen in the above example, it may not be possible to quantify the influences of stall or even detect their presence during such low pressure testing. Therefore, it would be more advantageous to conduct rotating stall research using high pressure test vehicles.

Diffuser Rotating Stall

Though this section is intended to address the entire subject of diffuser rotating stall, the primary focus will be on vaneless diffusers or the vaneless portion of vaned diffusers; i.e., the portion between the impeller and diffuser vanes (the "semi-vaneless space") or between the diffuser vanes and the downstream component (return bend or volute). Some comments on the vaneless portion are offered but the majority of the rotating stall problems encountered in vaned diffuser stages arise in the vaneless portion of those diffusers. Recall, problems associated with stationary stall in vaned diffusers were noted previously.

Vaned Diffusers

As noted, stall can occur in the vaned portion of a diffuser. The primary cause is leading edge incidence, though poor passage area distribution or vane design may also contribute. Regardless, the result will be flow separation from the vane surfaces or side walls. If the flow separation causes vortex shedding, this shedding may promote the formation of rotating diffuser stall in the vaneless space upstream of the diffuser vanes. Regardless of whether stationary or rotating, the disturbed flowfield can hinder the performance of downstream components, yielding higher losses and a reduction in operating range. The incidence or separation effects can also cause disturbances in the flowfield upstream of the diffuser vanes (backflow) or may, in fact, be the consequence of some upstream disturbances; i.e., impeller secondary flows, etc. In fact, it may be possible to cause rotating stall in the vaned portion of a diffuser if the diffuser follows an impeller that is experiencing rotating stall. Since the stall cells exiting the impeller will be rotational in nature, angular momentum will force the "cells" to rotate through the vaned diffuser. Of course, as the "cells" impact the diffuser vanes, they will likely be disturbed or even eradicated. In short, the diffuser vanes may actually serve to "wash out" impeller stall cells.

The stall may cause significant unbalanced forces on the rotor, especially when the vanes are closely coupled to the impellers (Sorokes and Welch, 1992) (Figure 22). Consideration must be given to the incidence swings that may occur as the end user operates the compressor. If it is clear that one or more of the required operating conditions result in high incidence; i.e., in excess of 10 degrees; there is a high probability that flow separation and the associated stall will occur.

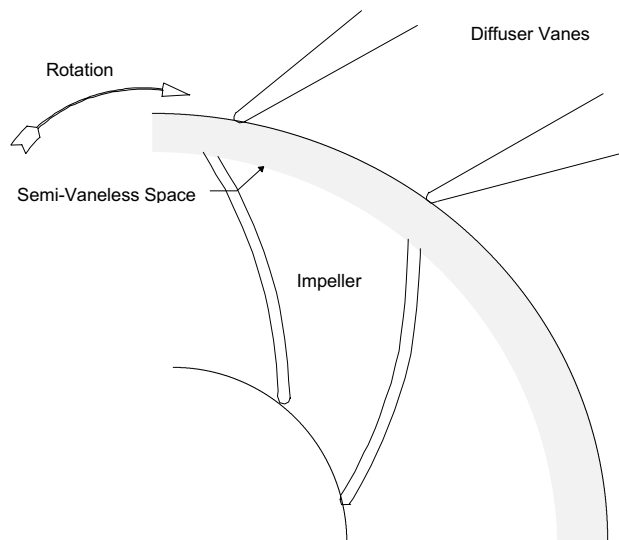


Figure 22. Spacing Between Impeller and Diffuser Vanes.

It is difficult to characterize the radial vibration frequencies that arise due to stall in the vaned portion of a diffuser. Unfortunately (or fortunately), there are limited data available in which stall was attributed directly to the vaned diffuser. Some have reported frequencies that are proportional to the number of impeller blades or diffuser vanes; i.e., blade or vane passing. Others (nearly all associated with low solidity vaned diffusers, LSDs) have cited subsynchronous frequencies in the same range as would be expected for stall in a vaneless diffuser. In the latter case, it has been speculated that the stall actually formed in the vaneless space between the impeller and diffuser due to either:

- Highly tangential vaneless space flow angles; or
- High levels of incidence leading to vortex shedding and stall cell formation.

Examples of Stall Associated with Vaned Diffusers

Despite building and testing a very large number of compressors that employed LSDs and other vaned types (i.e., wedge, airfoil, rib), the OEM has encountered very few cases of subsynchronous vibration or stall that were directly attributable to the diffuser. In the majority of these instances, the situation was rectified by restaggering the diffuser vanes; i.e., adjusting the vane inlet angles to better match the impeller exit flow conditions. The frequency spectra resulting from the inappropriate setting angles showed both subsynchronous (12 percent to 25 percent of running speed) and supersynchronous (blade/vane passing) components.

There have been two cases in which restaggering the diffuser vanes did not eliminate the subsynchronous vibrations. In these situations, the compressors were tested with one or more vaned diffuser arrangements and, finally, with vaneless diffusers. When the vanes were removed, the subsynchronous vibration was still apparent but at a reduced amplitude as compared to the test with the vanes installed. Consider the frequency spectra given in Figures 23 and 24. The spectrum in Figure 23 was taken during a near surge excursion with the LSDs installed. The spectrum shown in

Figure 24 was taken at the same flow condition after the LSDs were removed. Clearly, the amplitude was reduced when the LSD vanes were not present, yet a response was still evident. In short, the LSD vanes were serving as “reflectors” that amplified the effect of stall cells thought to be forming in the semi-vaneless space immediately outside the impeller exit. With the vanes in place, these stall cells or pressure disturbances were being reflected between the impeller and the diffuser vanes, causing unbalanced radial forces on the rotor. Without the vanes to serve as “reflectors,” the blade - vane interactions were eliminated and the rotor vibrations reduced.

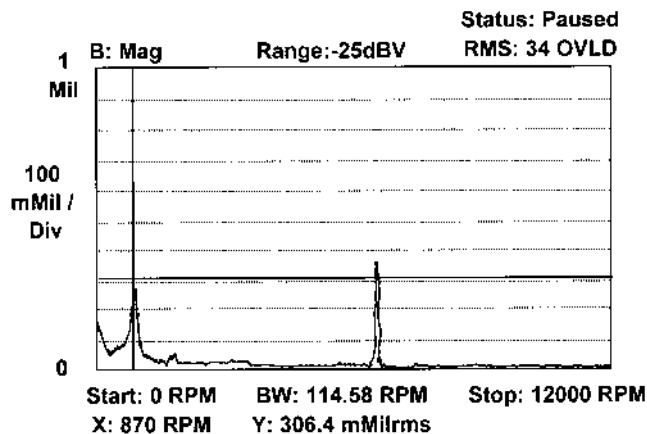


Figure 23. Radial Vibration Spectrum with LSDs Installed.

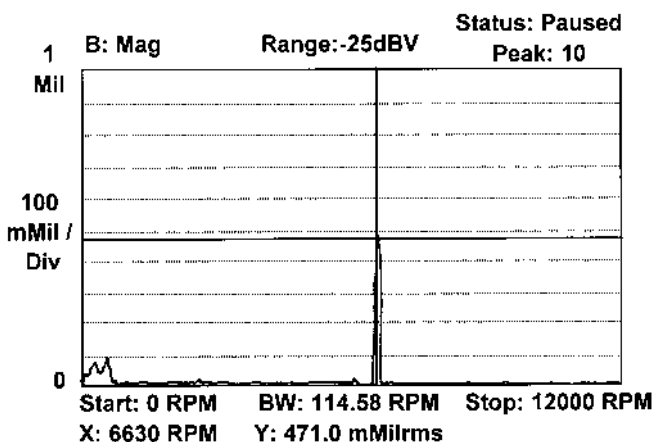


Figure 24. Radial Vibration Spectrum with LSDs Removed.

Calculations of the flow angles in the semi-vaneless space showed that, while incidence on the LSD vanes was minimal (i.e., approximately -2 degrees), the flow angles exceeded the critical angle for vaneless diffuser stall (more detail in following sections). The calculations supported the contention that the stall was occurring upstream of the LSD vanes.

The diffuser passages were contracted to move the flow angle out of the stall regime and new LSD vanes were designed to match the more radial flow angles. Upon retesting the compressor, no subsynchronous vibrations were encountered at any flow condition within the required operating range.

In summation, vanned diffusers can be the source of stall-related phenomena; the result of high levels of positive or negative incidence. They can also accentuate vibration resulting from stall cells rotating in the semi-vaneless area between the impeller and vanned diffuser. The designer must be aware of these critical factors and ensure that vane incidence and/or vaneless flow angles remain within acceptable limits.

Vaneless Diffusers

Some of the earliest research into vaneless diffuser rotating stall was conducted by Dr. Willem Jansen (1964). Jansen was investigating stall in vaneless diffusers caused by localized nonuniformities in the radial gas velocity. He determined that these nonuniformities lead to pressure disturbances or “stall cells” that rotate circumferentially around the compressor, subjecting the rotor to unbalanced pressure forces. Jansen’s work showed that the onset of diffuser rotating stall was most strongly influenced by the diffuser flow angle. Once the diffuser angle exceeded some critical angle, rotating stall occurred. Depending on the flow conditions and the details of the diffuser geometry, single or multiple stall cells (i.e., two, three, four, etc.) can form. The rotor vibration characteristics will be a function of this number of cells and their rotational speed relative to the compressor operating speed.

The flow angle in a diffuser is a function of operating conditions as well as the details of the diffuser geometry. Jansen’s studies showed that the critical angle for the onset of rotating stall is also a function of the diffuser geometry and the gas Reynolds Number. To aid designers in their efforts to avoid rotating stall, Jansen developed a series of guidelines or correlations that showed how the critical angle would change for various diffuser geometries and Reynolds numbers (Figure 25).

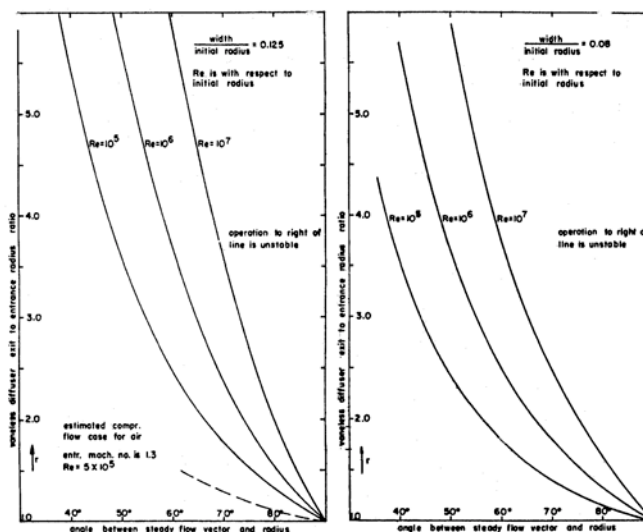


Figure 25. Jansen Criteria for Rotating Stall Avoidance in Vaneless Diffusers.

Subsequent research into rotating stall sought to further refine these guidelines or correlations. Among these were the efforts of Senoo and Kinoshita (1977, 1978), Senoo, et al. (1977), Abdelhamid (1980, 1985), Abdelhamid and Bertrand (1980), Abdelhamin, et al. (1979), and Frigne and Van den Braembussche (1984). Y. Senoo published several papers in the late 1970s that included criteria that became widely accepted by the compressor industry. Professor Senoo had sought to identify other parameters that influenced the critical angle for diffuser stall. He found that Mach number, Reynolds number, radius ratio, contraction ratio (ratio of diffuser width to impeller tip width), and, most notably, velocity distortion at the diffuser inlet all played an important role in determining the critical angle. This latter parameter is quite important because it suggests that the more disturbed the impeller exit flow profile, the greater the likelihood that the downstream diffuser will stall.

Kobayashi, et al. (1990), and Nishida, et al. (1988), expanded on the Senoo work, investigating the effects of diffuser inlet profile on Senoo’s criteria. They found that the rate of diffuser pinch and the general shape of that pinch (i.e., the diffuser hub and shroud entrance geometry) can have significant influence on the accuracy

of the Senoo methods. Interestingly, their work showed that rotating stall could occur at higher flow (i.e., more radial flow angles) if there is excess area above the impeller exit. This situation seems to be more critical in lower flow coefficient stages. Sorokes (1994) supported this contention in his work based on CFD analyses of various diffuser entrance geometries.

Despite all the published literature and ongoing research (notably the Concepts ETI rotating stall consortium), like impeller rotating stall, there remains no definitive set of criteria for rotating stall avoidance in vaneless diffusers. However, experience has shown that conservative application of the Senoo criteria yields a very high rate of success in avoiding diffuser stall. For example, insuring that the diffuser flow angles do not come within three to five degrees of the critical angle based on the Senoo criteria typically will ensure rotating stall avoidance in most cases (Figure 26). Of course, it is crucial that the flow angles be assessed over the entire required operating range for the compressor; i.e., from design flow back to the surge control line.

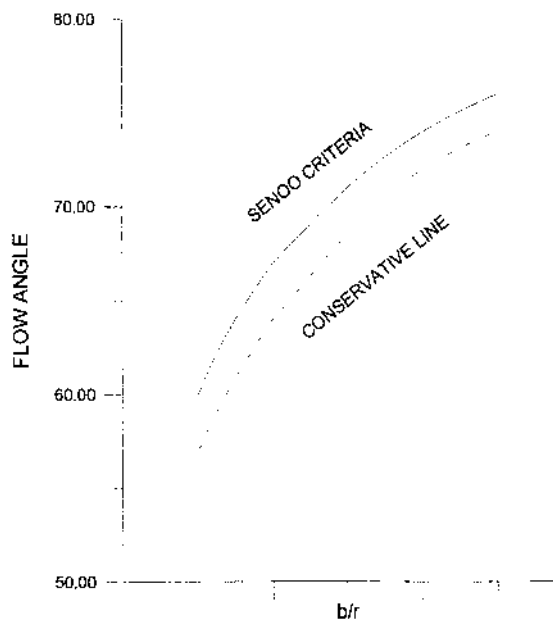


Figure 26. Senoo Criteria for Stall Avoidance Showing Conservative Line.

Vaneless Diffuser Rotating Stall Characteristics

Compressors experiencing subsynchronous vibration due to diffuser rotating stall exhibit some or all of the following characteristics:

- The subsynchronous radial vibration frequency is in a range of 6 percent to 33 percent of running speed.
- The vibration frequency is sensitive to flow rate and, after onset, will typically increase as the flow rate is reduced.
- The vibration frequency tracks with speed as long as Q/N is held fairly constant.
- There is a hysteresis zone associated with the onset flow rate. That is, when reducing flow, the phenomenon will appear at some flow rate. However, the vibration does not disappear simply by moving back above that flow rate. Instead, operators have to increase flow significantly beyond that rate to “wash out” the stall cells.
- There may be sudden jumps in frequency as the stall progresses from one to two to three cells, etc.
- If dynamic pressure probes are available, their output shows a response in the 6 percent to 33 percent range. They also show a

frequency spectrum consisting of numerous harmonics of some basic frequency. The spectrum appears as would a “clipped square wave.”

Examples of Stall Associated with Vaneless Diffusers (or Vaneless Passages)

- **Vaneless Diffuser**—Rather than cite specific compressors that experienced diffuser rotating stall, this section provides an overview of the two most common reasons that the phenomenon arises in industrial turbomachinery. This section also describes how a stall can form in other vaneless portions of the flow passage and addresses two examples of such.

Vaneless diffuser rotating stall can occur if designers do not account for assembly tolerances within a compressor. Another common reason is improper calculation of the upstream impeller exit flow angle causing an inaccuracy in specification of the diffuser width necessary for stall avoidance. That is, the calculated impeller exit flow angle is more radial than in actuality, resulting in insufficient diffuser pinch and a diffuser flow angle that is too tangential.

Returning to the subject of assembly tolerances, it is common practice to allow machining or assembly tolerances on the parts (return channels, guide vanes, inlets, discharge volutes) that stack together to form the compressor flowpath. When the unit is operated, any gaps between components (created by the machining or assembly tolerances) will be closed as the pressure builds on the walls of the various flow passages. All walls will deflect away from the point of highest pressure within the machine. In a compressor, the highest static pressure occurs in the last stage diffuser. Therefore, the walls of that diffuser will move apart as any machining or assembly gaps present in the remaining components are closed. Failure to account for the growth of this diffuser width can have significant consequences.

Most past occurrences of diffuser rotating stall encountered by the OEM were caused by the deflections described above. At operating pressures, walls deflected, the last stage diffuser width increased, the diffuser flow angle increased (became more tangential), and rotating stall developed. The machines exhibited low frequency subsynchronous radial vibrations in the range of 6 percent to 33 percent of the running speed, though the majority fell in a 6 percent to 18 percent range. The excess vibration typically arose as operators throttled the compressor toward the surge control line and, once present, would remain until the compressor was moved to much higher flow rates. Again, since the vibrations come and go at different flow rates, the phenomenon is said to have a hysteresis zone.

In all but limited cases, the stall was eliminated by reducing the diffuser widths such that, at pressure, the deflections would not result in flow angles that reached the critical level necessary to instigate rotating stall (refer to Figure 27 for typically corrective measure). It is clear that manufacturing tolerances and material deflection under pressure must be accounted for to ensure stall avoidance.

In a small number of cases, rotating stall was eliminated by installing low solidity vaneless diffusers. Such diffusers delay the onset of rotating stall by influencing the growth of secondary flows and boundary layers that promote stall inception. LSDs are a more attractive option when dealing with low flow coefficient stages. In such cases, the amount of vaneless diffuser pinch necessary to ensure proper flow angles often would produce unacceptable efficiency loss. The LSD eliminates this concern by allowing stable flow to be maintained with wider passages. Of course, in designing the vaneless diffuser, one must avoid creating different forms of stall caused by vane incidence effects. (Refer to *Vaned Diffusers* above.)

- **Return Bend**—Another form of vaneless space rotating stall can occur in the return bend (the 180 degree bend between the diffuser exit and return channel entrance, Figure 28) as reported by Sorokes, et al, (1994). Though not typically considered part of the

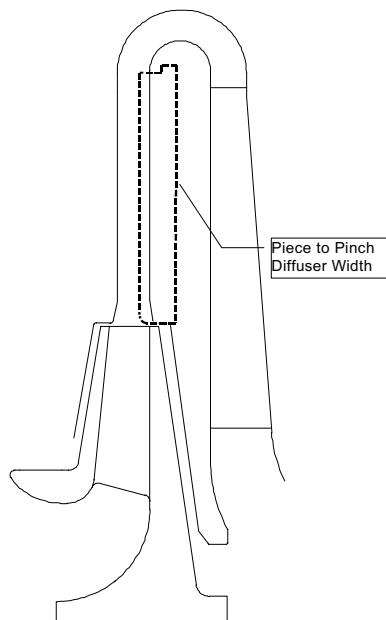


Figure 27. Typical Diffuser Correction.

diffuser, the return bend does constitute a vaneless space and, therefore, is a potential location for stall inception. In fact, since area typically increases through the 180 degree bend, there is a greater tendency for secondary flows to arise and form rotating stall cells. Little or nothing can be found in the open literature regarding rotating stall in this element. However, there has been strong evidence for such in at least two instances.

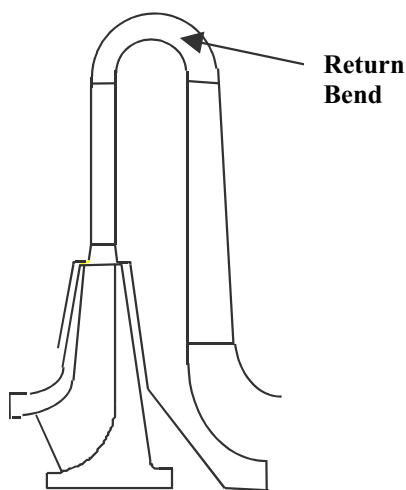


Figure 28. Return Bend (Vaneless Space).

In both cases, the return bend designs fell within previous experience, implying that there was little reason to suspect any potential for stall. In addition, the diffuser widths upstream of the bends were very conservatively sized to avoid rotating stall. Similarly, the impellers adhered to all known criteria for stall avoidance. Therefore, it was very surprising when subsynchronous radial vibrations arose. The subsynchronous frequency was in the range characteristic of vaneless diffuser stall. The frequency spectra and waveforms also bore a strong resemblance to those generated by diffuser rotating stall.

A review of the flow angles in the various stage components identified rather high tangential angles in the return bend passages. While the diffuser flow angles were well below the critical level for rotating stall, the flow angles in the return bend were not. In short,

despite having no prior experience with stall in a return bend, the data indicated that the stall was occurring in the bends and not in the diffuser passage.

In the first of the two cases, the stall was eliminated by reducing the return bend passage widths in all stages. In this instance, the diameter to the entrance of the bends was not changed; implying no change in the tangential velocity component. The decreased passage width effectively increased the meridional velocity and, therefore, reduced the gas flow angle.

In the second compressor, in addition to a reduction in cross-sectional passage width, the radius to the entrance of the return bend was decreased. The change in radius and passage area caused both the gas tangential and meridional velocity to increase. However, the meridional velocity, being a function of both the radius and the passage width, increased by a larger percentage than did the tangential velocity. The result was a decrease in gas flow angle of approximately five degrees at any given flow condition. As with the first case, the stall and associated subsynchronous radial vibration were eliminated from this compressor.

In these two cases, the machines exhibited characteristics that could have been interpreted as diffuser rotating stall, yet the stall was not caused by the diffusers. Without careful review of all the geometry and available data, analysts may target the wrong components for corrective measures.

Because of these experiences, it is now common practice to assess the flow angles through return bends using much the same criteria as applied for vaneless diffusers. Logic suggests that if the flow angles are too tangential for a vaneless diffuser, they should likewise be too tangential for a vaneless return bend.

Interaction "Stall"

Nonuniform pressure fields can be formed through the interaction of components or the interaction of the pressure fields created by adjoining components. It is not clear that these phenomena should be characterized as rotating stall. Still, they do cause a rotating nonuniform pressure field that imposes unbalanced forces on the rotor and their influence on said rotor mimic those of true rotating stall. Therefore, it is appropriate to associate these phenomena with rotating stall.

Impeller - Diffuser Interaction

The most common form of impeller - diffuser interaction occurs when one wall of a diffuser abruptly overlaps the impeller exit gas passage, causing an obstruction in the flowpath. The flow impinging on the obstruction causes pressure disturbances that can influence the rotor. Such a situation can be avoided by proper flaring of the diffuser entrance, thereby ensuring that detrimental overlap cannot occur. Of course, one must be cognizant of the axial movement of the rotor during operation at various flow conditions.

Not surprisingly, this form of interaction stall is more prevalent at the high flow end of the compressor performance map. At such flow rates, the impeller exit flow angle is more radial and there is more kinetic energy in the gas stream. Consequently, the energy involved in the interaction is higher, resulting in greater forces acting on the rotor. Further, as one reduces flow and the angle becomes more tangential, it is easier for the flow to "slip around" the obstruction without causing feedback to the rotor.

There are no generally accepted characteristics for impeller - diffuser interaction stall. However, the following loose criteria are offered:

- The frequency range is approximately 20 percent to 50 percent(?) of running speed.
- There is no hysteresis zone.
- The frequency is sensitive to flow rate but may not appear sensitive to speed.
- There is a greater tendency for this phenomenon to occur at high rather than low flow rates.

Diffuser Volute Interaction

A second form of interaction stall that has gained interest in the turbomachinery world is interaction between the diffuser and the discharge volute. Some hold that this form should be lumped under vaneless diffuser stall since the phenomenon is caused by interaction of diffuser stall cells (or the rotating nonuniform static pressure field) with the volute tongue (or tongues). As with all other forms of stall, the result is unbalanced pressure forces on the rotor, leading to rotor vibrations.

What makes this form of interaction stall so troublesome is that it can easily be misinterpreted as impeller stall because of the frequencies involved. Recall that diffuser stall is characterized by frequencies in the 6 percent to 33 percent of running speed range. Suppose now that there are three diffuser stall cells (or three lobes in the pressure field) rotating at 20 percent of running speed. These “cells” will each interact with the volute tongue in one revolution of the pressure field. Since sensitive to the interaction of each “cell” with the tongue, the rotor response will be at three (the number of “cells”) times the rotational frequency of the pressure field (20 percent of running) or 60 percent of running speed. The analyst might be misled into believing the problem is impeller stall. However, since rooted in diffuser rotating stall, the phenomenon will exhibit a hysteresis zone, thus distinguishing it from impeller stall.

Other Components

Since rotating stall is the consequence of any nonuniform pressure field rotating within the compressor, anything that contributes to the formation of such nonuniform fields can cause some form of rotating stall. Possible contributors include:

- Flow in impeller recess areas (the cavities that surround the rotating impellers),
- Eccentric rotors (area varies circumferentially causing flow velocities to vary resulting in nonuniform static pressure), and
- Nonuniform pressure fields caused by inlets, volutes, sidestreams, etc.

In short, any flow carrying passage within a compressor (Figure 29).

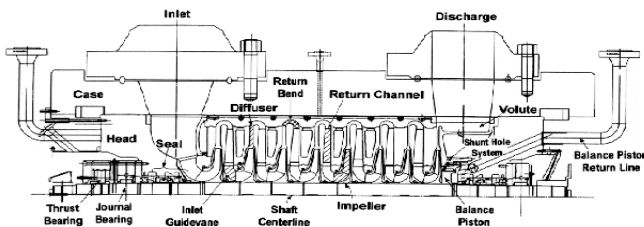


Figure 29. Compressor Cross-Section.

It would be nearly impossible to characterize all the frequencies, waveforms, etc. that could result from the anomalies listed above. Suffice to say, if the more common phenomena (impeller and diffuser stall) can be effectively eliminated from consideration, one must look elsewhere for the source of the forces causing subsynchronous vibration.

VIBRATION SIGNALS

Each of the various types of vibration signals one might see are discussed below. It is assumed that an FFT signal analyzer is available, to put the signal in the frequency domain. Although the best way to visualize and describe these signals with such an analyzer is to view them in real time, a reasonable alternative is to view a series of snapshots of the signals at varying times. This is preferable to the often used “peak hold” mode of the typical analyzer, since it does not hide the variation in amplitudes and frequencies that are occurring at levels underneath the maximum amplitudes.

Free Vibration

As noted earlier, “free” vibration is typically seen only as what is commonly called “rotor instability.” A typical example is shown in Figure 30. The frequency of interest (66 to 72 Hz in this case) is the first natural frequency of the rotor. The signal appears at a relatively low amplitude initially (top spectrum in Figure 30), but increases in amplitude as an operating parameter such as discharge pressure is increased, until it increases dramatically on its own, without changes in operating conditions. Eventually, the vibrations reach trip level (bottom spectrum in Figure 30) and the unit shuts down.

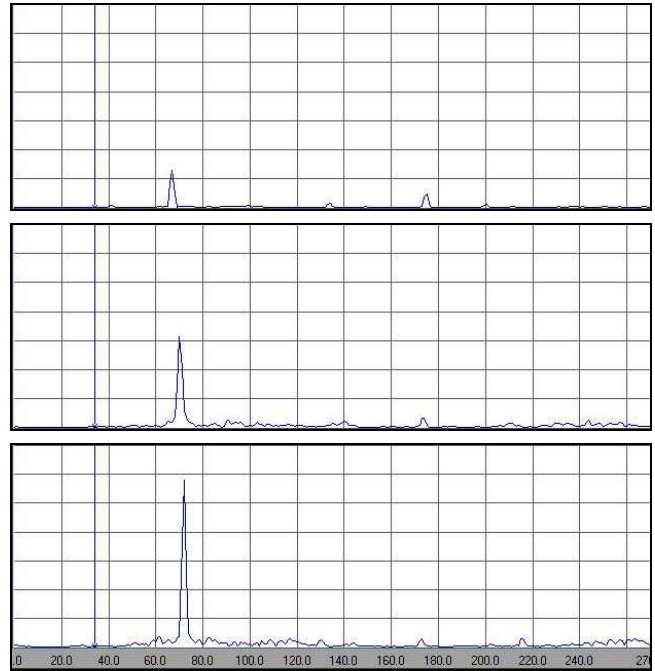


Figure 30. Spectra from Vibration Probe During Rotor Instability.

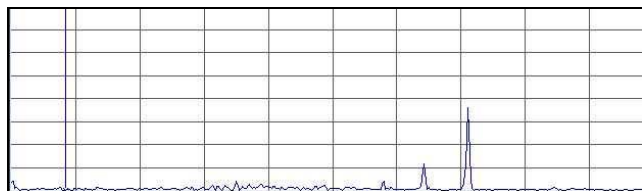
In this particular case, although no speed change of consequence occurred to show the lack of relationship between the rotating speed and the natural frequency, the change in the natural frequency as it begins to increase and then dominate the vibration of the rotor, demonstrates its independence relative to the rpm. Also note the relative absence of components of the vibration at other frequencies. All one can see of consequence is the natural frequency and the running speed of the machine, which is the peak at 173 to 175 Hz.

Forced Vibration

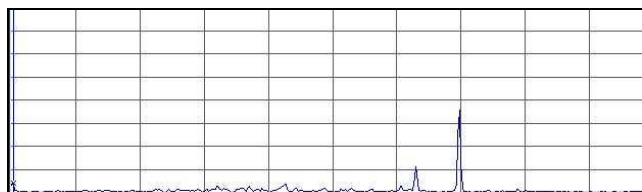
Harmonic Force

As discussed earlier, an impeller stall is a good example of a relatively clean single frequency subsynchronous harmonic force. In Figure 31 a signal is seen at 117 to 128 Hz due to such a stall. The unit is running at 130 to 142 Hz, as indicated by the larger synchronous vibration signal. Note that the subsynchronous signal stays at a constant 89 to 90 percent of the running speed, changing frequency with changes in speed from Figure 31a at 142 Hz running speed, to Figure 31b at 140 Hz, and Figure 31c at 130 Hz running speed. Other characteristics of note are the relatively steady amplitude at the stall frequency, and the lack of other significant components of the vibration.

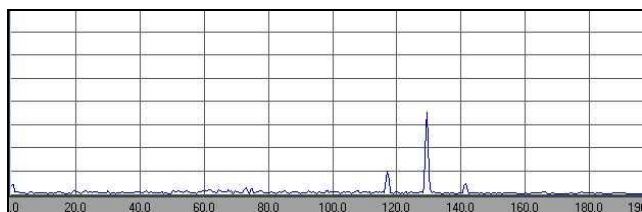
Figure 32 illustrates the freedom of harmonics in this vibration signal. The same unit is running at 150 Hz in this instance, with the stall frequency at 134 Hz. The frequency scale is set at three times the running speed, making it evident that no multiples of the stall frequency are present, at least at noticeable amplitude levels, in the



(a) 142 Hz running speed



(b) 140 Hz running speed



(c) 130 Hz running speed

Figure 31. Variation in Subsynchronous Vibration Frequency with Running Speed.

vibration signal. Other characteristics specific to impeller stall, such as the lack of hysteresis when changing flow, and the ability to make the signal disappear by flow reductions (changing numbers of stall cells) are difficult to present without live presentations of the data.

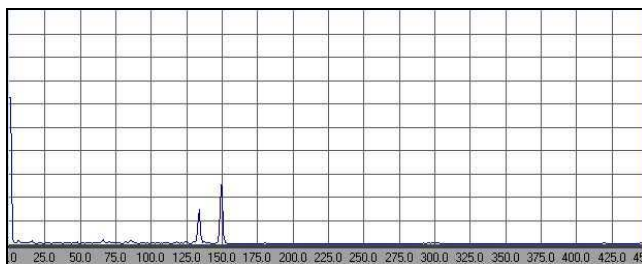


Figure 32. Radial Vibration Spectrum During Impeller Stall.

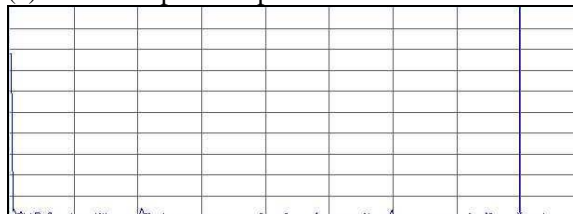
Periodic Force

Impeller and diffuser stall are both good examples of periodic forces. As noted previously, the pressure disturbances caused during stall rotate at speeds lower than the rotor, resulting in subsynchronous radial vibrations. Typical frequency spectra for impeller and diffuser stall are given in Figures 33 and 34, respectively. In each figure, the top trace (a) is the vibration probe signal immediately prior to onset of the stall. The second trace (b), also taken just prior to the onset of stall, is from a dynamic pressure transducer in the diffuser immediately outside the impeller for the impeller stall case or at the exit of the diffuser in the diffuser stall case. The third trace (c) is from the vibration probe after onset of stall and the fourth trace (d) is the dynamic pressure transducer output after onset.

Clearly, in the case of impeller stall (Figure 33), forced vibration is only occurring due to the stall at 133 Hz. Also note that the $1\times$ frequency (149 Hz) does not appear in the dynamic pressure probe output.



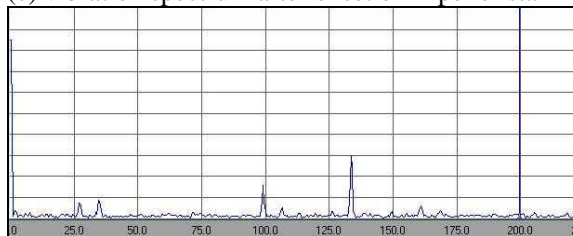
(a) vibration spectrum prior to onset



(b) dynamic pressure spectrum prior to onset



(c) vibration spectrum after onset of impeller stall



(d) dynamic pressure spectrum after onset of impeller stall

Figure 33. Vibration and Dynamic Pressure Spectra Before and After Onset of Impeller Rotating Stall.

Note that there are multiple harmonics (4.5 Hz, 9.0 Hz, 13.5 Hz, etc.) in the dynamic pressure spectra in Figure 34(d). In this case, the probe was not sensing many cells moving at different speeds. Rather, the multiple peaks represent the FFTs rendition of the typical “clipped square wave” appearance of a diffuser stall waveform, which leads to multiples (harmonics) of the base frequency (4.5 Hz).

Also note that although the pressure signal in Figure 34(d) indicates multiple frequencies present, on the vibration response in Figure 34(c) only the primary and first multiple are evident, at the same frequencies as in the pressure signal. This vibration response is larger at the lower frequencies due to high damping in the system, with relatively low stiffness. Such a result is evident from solutions of simple systems, as shown in Equation (11) above. As indicated, when damping is a significant factor in the response equation, amplitude response for the same force will increase as the frequency is reduced. The high damping values that minimize dangerous vibration response at higher frequencies allow greater response at the low frequencies of this example. In fact, the highest response is at the lowest frequency, while the forcing function is greater at a higher frequency.

In the aero section introduction, emphasis was placed on the difference between surge and stall. To illustrate the difference, consider Figure 35. The trace in Figure 35(a) is from a dynamic pressure transducer in a diffuser passage when said diffuser is in a rotating stall mode. The trace in Figure 35(b) was taken while the same machine was in true surge. Note the extremely low frequencies associated with the surge (approximately 1 Hz).

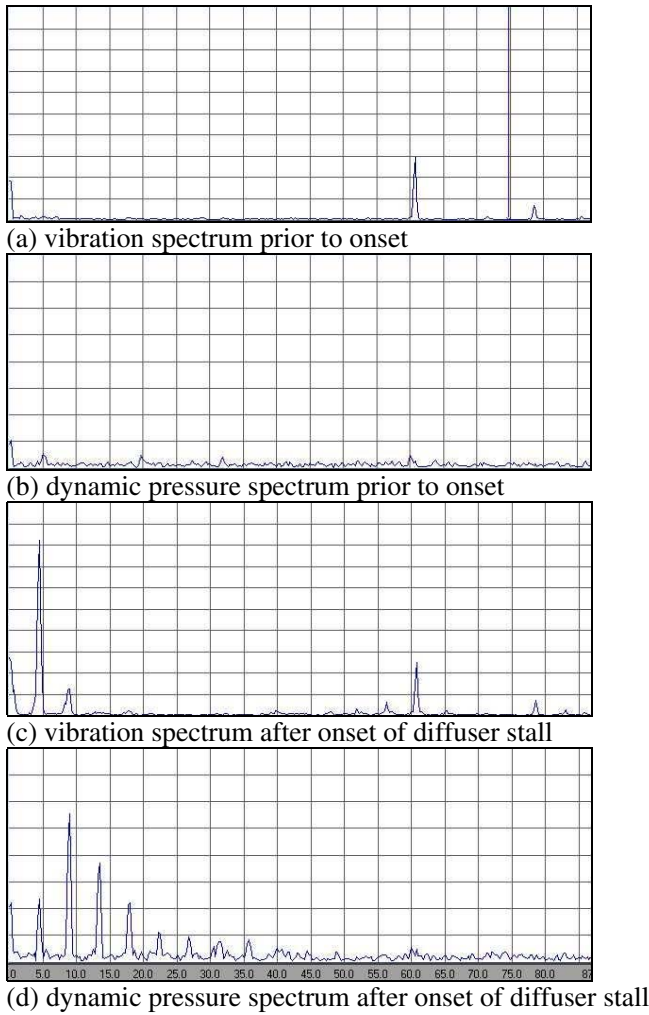


Figure 34. Vibration and Dynamic Pressure Spectra Before and After Onset of Diffuser Rotating Stall.

The associated raw waveforms for the stall and surge are given in Figure 36. Frequency spectra for the vibration probes under the same conditions (stall and surge) are shown in Figure 37. The distinctions between the two conditions are fairly obvious. Note that surge results in a broad impulse excitation of the rotor that may or may not excite the first natural frequency, depending on the amount of damping in the system, whereas the response to stall is primarily at the stall propagation frequency.

Of course, one must be very careful when attempting to identify the cause of low order subsynchronous vibrations. Other forces acting on the rotor can reflect frequency spectra and/or waveforms like those of the various aerodynamic phenomena. For example, the frequency spectra shown in Figure 38 might be mistaken for diffuser stall. The spike at 63 Hz is the $1\times$ response while the spike or spikes at lower frequencies (5 Hz in Figure 38a; 4.5 Hz and 6.75 Hz in Figure 38b) are the subsynchronous response. Clearly, the subsynchronous frequencies are in the classic range for diffuser stall. However, the shift in the subsynchronous peak occurs at constant flow conditions. In fact, the subsynchronous vibration in this case is caused by a “rattling” seal ring and not by any aerodynamic phenomena. Oil seal rings designed for high pressures may not “seat” properly on the end face at lower pressure test conditions, allowing oil to flow around the seal ring, not just under it. This causes the rattle, which is easily uncovered by adjustments in seal oil pressure. Onset is usually sudden, but as oil pressure is increased, the vibration amplitude will decrease, and the frequency will increase.

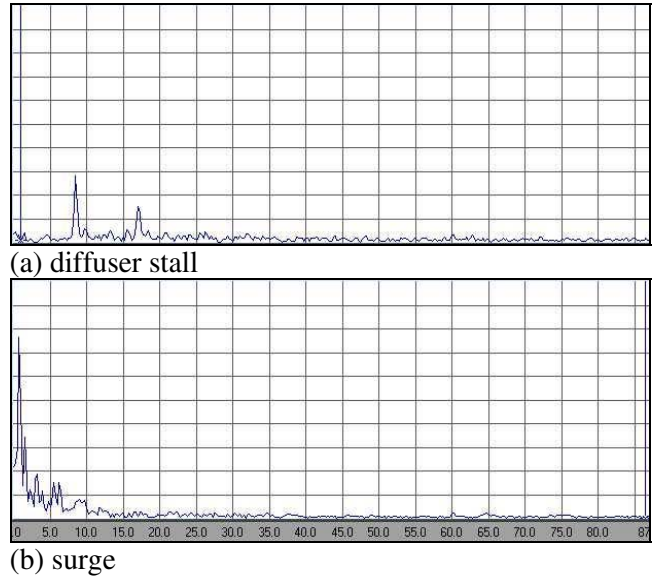


Figure 35. Dynamic Pressure Spectra—Stall Versus Surge.

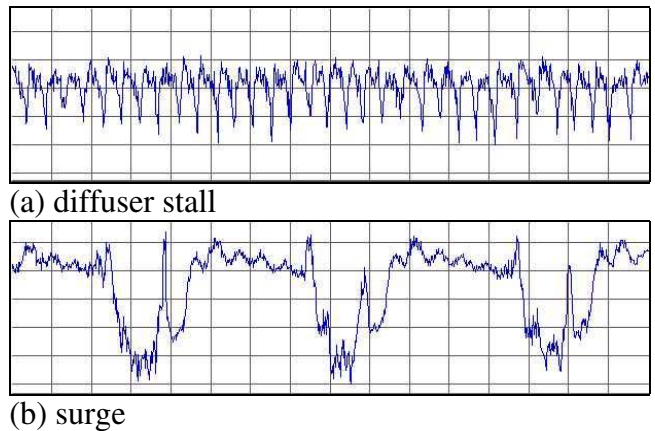


Figure 36. Dynamic Pressure Waveforms—Stall Versus Surge.

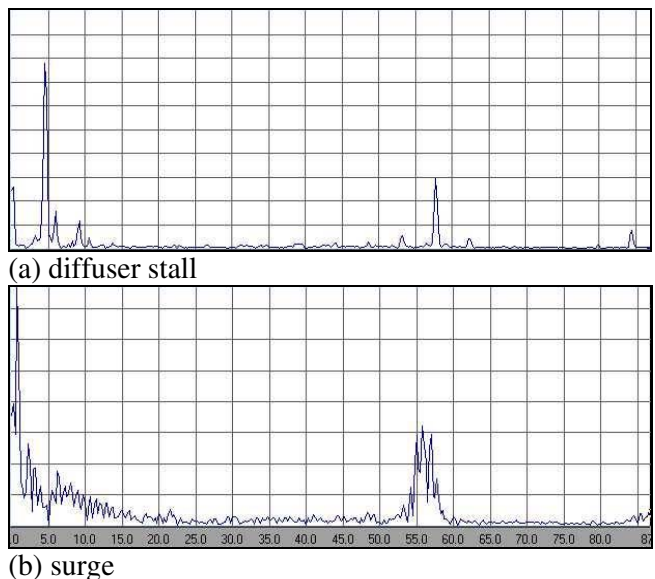
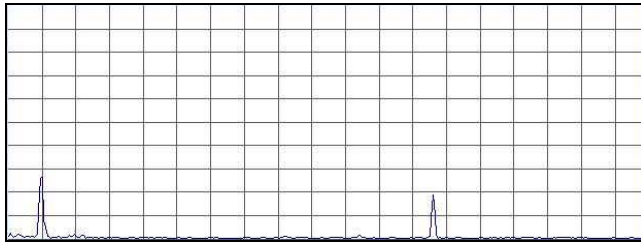
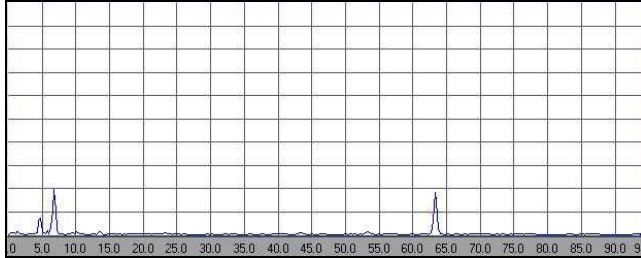


Figure 37. Vibration Spectra—Stall Versus Surge.



(a) lower seal oil pressure



(b) higher seal oil pressure

Figure 38. Vibration Spectra—"Rattling" Seal Ring.

Arbitrary Aerodynamic Forces

Due to its transient nature, vibration caused by arbitrary forces is very difficult to capture on a sheet of paper. It may be most useful to compare a typically used "peak hold" spectrum with other both specific and random spectra for the same signal. The peak hold spectrum shown in Figure 39 is from 100 seconds of data with a rotor undergoing such forces. It clearly indicates a peak response to these forces just below 25 Hz, at the natural frequency of the unit, with the other major amplitudes at the running speed and at very low frequencies where the high system damping results in high response levels (refer to earlier comments). Though all levels shown were within specification requirements, the peak at the first natural frequency could be a cause of concern if this plot is just used for evaluation. More investigation is needed to determine the true nature of the vibration.

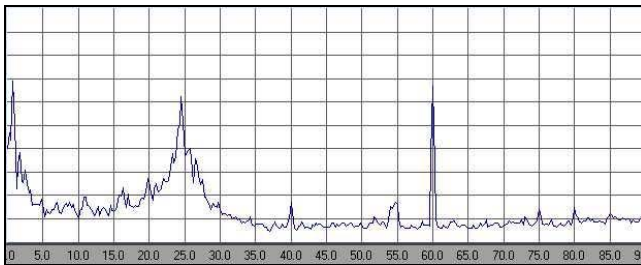
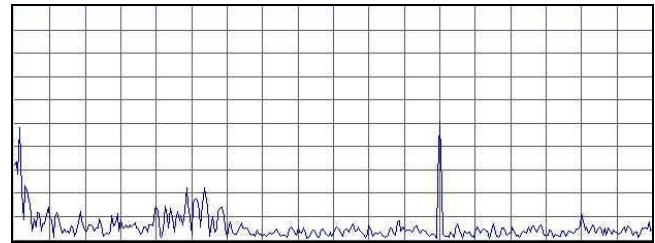
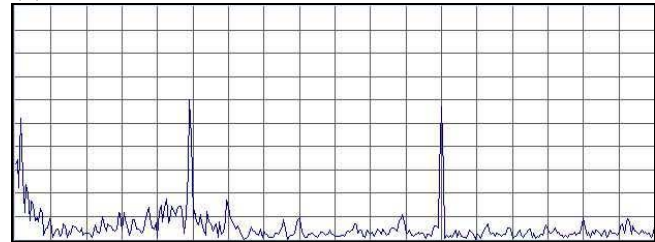


Figure 39. Peak Hold Vibration Spectrum—Arbitrary Aerodynamic Forces.

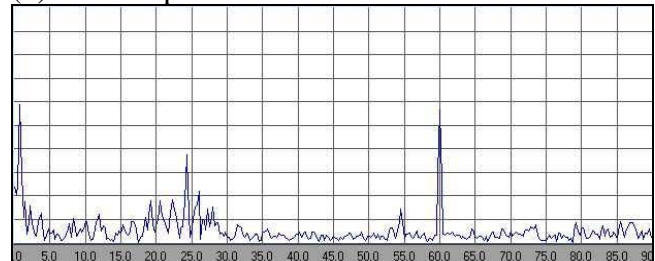
Figure 40 indicates the vibration spectrum at the time of the highest amplitude at the first natural frequency, as well as the spectrum two seconds before and two seconds after. Figure 41 indicates the spectrum at 10, 30, and 60 seconds after the peak signal. These data show the transient nature, varying amplitude, and varying frequencies typical of response to arbitrary forces. If viewed in real time, such a spectrum would appear to be "dancing" or "rumbling," with amplitude peaks highest in the area of the rotor first natural frequency (approximately 40 percent of running speed). No "fixed spikes" exist at any frequency, and the various peaks form and disappear in time, shifting in both amplitude and frequency with no apparent correlation to any operating parameters (i.e., flow rate, speeds, gas conditions, etc.). This is clear evidence of a forced vibration, with the rotor acting in response to external forces within the gas path.



(a) 2 seconds before

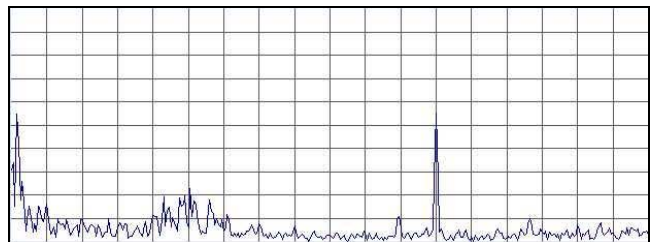


(b) Peak amplitude

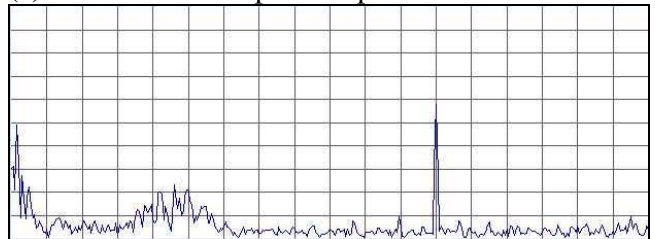


(c) 2 seconds after

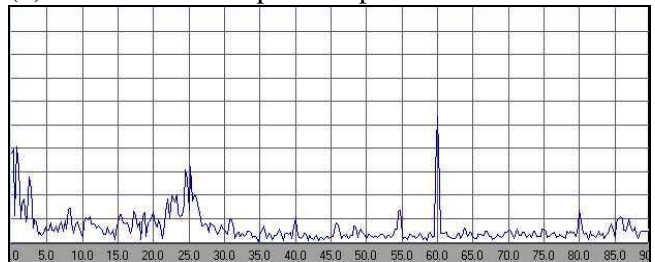
Figure 40. Vibration Spectra—Arbitrary Aerodynamic Forces.



(a) 10 seconds after peak amplitude



(b) 30 seconds after peak amplitude



(c) 60 seconds after peak amplitude

Figure 41. Vibration Spectra—Arbitrary Aerodynamic Forces (10, 30, and 60 Seconds After Peak Amplitude).

CONCLUSIONS

The forces acting within centrifugal compressors can cause a variety of responses in the rotor system. A general discussion of compressor rotordynamic behavior was presented including discussions on free and forced vibrations. Distinctions were made between significant subsynchronous vibration characteristics, such as rotor instability, and aerodynamically forced vibration of various types. Ways to distinguish between these various causes using vibration data were also provided.

The various aerodynamic phenomena that contribute to increased radial vibrations were discussed including impeller stall, diffuser stall, and interaction "stall." A general description of the flow physics was provided as were the commonly held identification criteria for each. Finally, various frequency spectra and waveform plots were offered to illustrate how the various phenomena may appear in vibration or pressure pulsation data; i.e., on a spectrum analyzer or oscilloscope.

No single paper can adequately address the entire subject of aerodynamic excitation of rotor systems. Still, it is hoped this document provides the reader with a good general overview of a very complex subject.

REFERENCES

- Abdelhamid, A. N., 1980, "Analysis of Rotating Stall in Vaneless Diffusers of Centrifugal Compressors," ASME Paper No. 80-GT-184.
- Abdelhamid, A. N., 1985, "Dynamic Response of a Centrifugal Blower to Periodic Flow Fluctuations," ASME Paper No. 85-GT-195.
- Abdelhamid, A. N. and Bertrand, J., 1980, "Distinction Between Two Types of Self-Excited Gas Oscillations in Vaneless Radial Diffusers," Transactions ASME Journal of Turbomachinery, *109*, (1), pp. 36-40.
- Abdelhamid, A. N., Colwill, W. H., and Barrows, J. F., 1979, "Experimental Investigation of Unsteady Phenomena in Vaneless Radial Diffusers," ASME Paper No. 78-GT-23, Transactions ASME Journal of Engineering for Power, *101*, (1), pp. 52-60.
- Frigne, P., Van den Braembussche, R., 1984, "Distinctions Between Different Types of Impeller and Diffuser Rotating Stall in a Centrifugal Compressor with Vaneless Diffuser," ASME Paper No. 83-GT-61; Transactions ASME Journal of Engineering Gas Turbine and Power, *106*, (2), pp. 468-474.
- Jansen, W., 1964, "Rotating Stall in a Radial Vaneless Diffuser," ASME Paper No. 64-FE-6, Transactions ASME Journal of Basic Engineering, pp. 750-758.
- Kobayashi, H., Nishida, H., Takagi, T., and Fukushima, Y., 1990, "A Study on the Rotating Stall of Centrifugal Compressors," (Second Report, Effect of Vaneless Diffuser Inlet Shape on Rotating Stall) Transactions of JSME (B Edition), *56*, (529), pp. 98-103.
- Nishida, H., Kobayashi, H., Takagi, T., and Fukushima, Y., 1988, "A Study on the Rotating Stall of Centrifugal Compressors," (First Report, Effect of Vaneless Diffuser Width on Rotating Stall), Transactions of JSME, *54*, (499), pp. 589-594.
- Senoo, Y. and Kinoshita, Y., 1977, "Influence of Inlet Flow Conditions and Geometries of Centrifugal Vaneless Diffusers on Critical Flow Angles for Reverse Flow," Transactions ASME Journal of Fluids Engineering, pp. 98-103.
- Senoo, Y. and Kinoshita, Y., 1978, "Limits of Rotating Stall and Stall in Vaneless Diffusers of Centrifugal Compressors," ASME Paper No. 78-GT-19.
- Senoo, Y., Kinoshita, Y., and Ishida, M., 1977, "Asymmetric Flow in Vaneless Diffusers of Centrifugal Blowers," Transactions ASME Journal of Fluids Engineering, *99*, (1), pp. 104-114.
- Sorokes, J. M., 1993, "The Practical Application of CFD in the Design of Industrial Centrifugal Impellers," *Proceedings of the Twenty-Second Turbomachinery Symposium*, Turbomachinery Laboratory, Texas A&M University, College Station, Texas, pp. 113-124.
- Sorokes, J. M., 1994, "A CFD Assessment of Entrance Area Distributions in a Centrifugal Compressor Vaneless Diffuser," ASME Paper No. 94-GT-90.
- Sorokes, J. M. and Welch, J. P., 1991, "Centrifugal Compressor Performance Enhancement Through the Use of a Single Stage Development Rig," *Proceedings of the Twentieth Turbomachinery Symposium*, Turbomachinery Laboratory, Texas A&M University, College Station, Texas, pp. 101-112.
- Sorokes, J. M. and Welch, J. P., 1992, "Experimental Results on a Rotatable Low Solidity Vaned Diffuser," ASME Paper No. 92-GT-19.
- Sorokes, J. M., Kuzdzal, M. J., Sandberg, M. R., and Colby, G. M., 1994, "Recent Experiences in Full Load Full Pressure Shop Testing of a High Pressure Gas Injection Centrifugal Compressor," *Proceedings of the Twenty-Third Turbomachinery Symposium*, Turbomachinery Laboratory, Texas A&M University, College Station, Texas, pp. 3-18.

BIBLIOGRAPHY

- Boncianni, L., Ferrara, P.L., and Timori, A., 1980, "Aero-Induced Vibrations in Centrifugal Compressors," Proceedings of Rotordynamic Instability Problems in High Performance Turbomachinery, Texas A&M University, NASA CP 2133, pp. 85-94.
- Fulton, J. W., 1986, "Subsynchronous Vibration of Multistage Centrifugal Compressors Forced by Rotating Stall," Proceedings of Rotordynamic Instability Problems in High Performance Turbomachinery, Texas A&M University.
- Japikse, D., 1996, *Centrifugal Compressor Design and Performance*, Concepts ETI, Inc., pp. 5/1-5/89.
- Kammer, H. and Rautenberg, M., 1985, "A Distinction Between Different Types of Stall in Centrifugal Compressor Stage," ASME Paper No. 85-GT-194.
- Seidel, U., Chen, J., Jin, D., and Rautenberg, M., 1991, "Experimental Investigation of Rotating Stall Behaviour Influenced by Varying Design and Operation Parameters of Centrifugal Compressors," Paper No. 91-Yokohama-IGTC-93.
- Sorokes, J. M., 1995, "Industrial Centrifugal Compressors—Design Considerations," ASME Paper No. 95-WA/PID-2.
- Thomson, W., 1965, *Vibration Theory and Applications*, Prentice-Hall, Inc.
- Timoshenko, S., Young, D., and Weaver, Jr., W., 1974, *Vibration Problems in Engineering*, John Wiley & Sons.
- Volterra, E. and Zachmanoglou, E., 1965, *Dynamics of Vibrations*, Charles E. Merrill Books, Inc.

ACKNOWLEDGEMENTS

The authors acknowledge the following individuals for their help in generating the figures and other presentation material used in this paper: Chuck Dunn, Jim Shufelt, Barry Clawson, Ed Thierman, and Dresser-Rand test stand personnel. We also thank Dresser-Rand for allowing us to publish this document.